Czech Technical University in Prague

department of instrumentation and control engineering

Master's Thesis

Parameter Identification and Filter Design for a Repetitive Controller of Hot Rolling Mills

Can Kutlu Yuksel

supervised by
prof. Ing Tomas Vyhlidal, Ph.D

Prague, 2019

CTU
CZECH TECHNICAL UNIVERSITY IN PRAGUE

MASTER'S THESIS ASSIGNMENT

I. Personal and study details

Student's name: **Yuksel Can Kutlu** Personal ID number: **473536**

Faculty / Institute: **Faculty of Mechanical Engineering**

Department / Institute: **Department of Instrumentation and Control Engineering**

Study program: **Mechanical Engineering**

Branch of study: **Instrumentation and Control Engineering**

II. Master's thesis details

Master's thesis title in English:

Parameter identification and filter design for a repetitive controller of hot rolling mills

Master's thesis title in Czech:

Identifikace parametrů a návrh filtru repetitivního regulátoru procesu válcování za tepla

Guidelines:

1. Perform state of the art in:
   i) parameter identification of low order time delay systems
   ii) control algorithms with time delay and eccentricity compensation in hot rolling processes
2. Design and implement an easy to apply algorithm for identification of rolling mill model parameters from process data
3. Propose a filter for a robust implementation of the repetitive internal model controller
4. Validate the algorithm robustness and analyze the results

Bibliography / sources:

[1] Omura, K., Ujikawa, H., Kaneko, O., Okano, Y., Yamamoto, S., Imanari, H., & Horikawa, T. (2015). Attenuation of roll eccentric disturbance by modified repetitive controllers for steel strip process with transport time delay. IFAC-PapersOnLine, 48(17), 131-136.

[2] Pietrzyk M. and Lenard J.: Thermal-Mechanical Modelling of the Flat Rolling Process. Series: Materials Research and Engineering, Springer-Verlag, Berlin, 1991.

[3] Skogestad, Sigurd, and Ian Postlethwaite. Multivariable feedback control: analysis and design. Vol. 2. New York: Wiley, 2007.

Name and workplace of master's thesis supervisor:

prof. Ing. Tomáš Vyhlídal, Ph.D., U12110.3

Name and workplace of second master's thesis supervisor or consultant:

Date of master's thesis assignment: **26.04.2019** Deadline for master's thesis submission: **12.06.2019**

Assignment valid until: ____________

prof. Ing. Tomáš Vyhlídal, Ph.D.
Supervisor's signature

Head of department's signature

prof. Ing. Michael Valášek, DrSc.
Dean's signature

III. Assignment receipt

The student acknowledges that the master's thesis is an individual work. The student must produce his thesis without the assistance of others, with the exception of provided consultations. Within the master's thesis, the author must state the names of consultants and include a list of references.

26-04-2019
Date of assignment receipt

Student's signature

Statement

I declare that I have worked out this thesis independently assuming that the results of the thesis can also be used at the discretion of the supervisor of the thesis as its co-author. I also agree with the potential publication of the results of the thesis or of its substantial part, provided I will be listed as the co-author.

Prague, 12.06.2019
Signature:

Acknowledgment

This work was supported by the Grant Agency of the Czech Technical University in Prague, grant No. SGS SGS17/176/OHK2/3T/12.

I would like to truly state my gratitude for my professor and supervisor prof. Tomas Vyhlidal. I have a deep regard for him due to his kindness and guidance.

None of the words is enough to express my gratitude to my lovely family and especially, to my mother. Thank you very much for your support.

Abstract: *In hot rolling mill products, periodic surface defects are encountered due to the inherent eccentricity present in the rolls. These defects can be considered as periodic disturbance to the system. To remove these defects, a controller design based on Repetitive Control method is investigated. By first approximating hot rolling mills from experimental data as first-order time delayed systems, the necessary controller conditions and properties that needs to be satisfied for periodic disturbance rejection are obtained for the particular type of systems with Internal Model Controller. Then with respect to these conditions, a methodology to obtain filters which hold a key part in Repetitive Control, is proposed and tested for its effectiveness and robustness in achieving successful control under disturbance and plant/model mismatch.*

Key Words: *Hot rolling mills, system identification, time-delayed systems, ARMAX, periodic disturbance control, eccentricity, Internal Model Control, Repetitive Control.*

Contents

List of Figures

List of Abbreviations

i, j	Complex number
w	Frequency
w_d	Frequency of disturbance
S{}	System
N	Number of clockwise encirclement
Z	Number of zeros
P	Number of poles
p_i	i^{th} pole
τ	Inherent time-delay of a system
θ	User-definable time-delay
arg()	Argument of a complex number or function
*	Convolution operator
k	Discrete-time index
t	Time
y[k]	Discrete-time signal
y(t)	Continuous-time signal
s	Laplace variable
X(s)	Transfer Function of system X and Laplace Transform of signal x(t)
T	Time Constant
ξ	Damping Ratio
K	Unit-step Gain
IMC	Intrnal Model Control
ARMAX	Auto Regressive Moving Average with Extra Input
ROP	Relative Order of Plant

Part I

Theory & Objectives

1 A Concise Review of Hot Rolling Mills and Statement of Problem

Hot rolling mills hold an important part of steel production and their production quality directly effects the reliability of further processes of the product. In spite of their wide usage in industry, hot rolling mills are exposed to many disturbances that reduce the effectiveness of the production method. Some of the sources of the disturbances like eccentricity in the rollers, are present inherently in hot rolling mills and their attenuation is achieved by introducing new systems to the milling stands. Hence, the enhancement of the product quality for hot rolling mills is a continuous demand.

Hot rolling mills are machines where hot rolling process is realized and rolling is a metal forming procedure which takes a stock of metal to reduce its thickness to a desired value. According to the temperature of the rolled metal, the rolling process is classified into two classes, namely, hot and cold. If the metal temperature is above the metals' re-crystallization temperature, then the process is classified as hot rolling. Conversely, if it is below the re-crystallization temperature, it corresponds to the cold rolling. The resulting products of a rolling are usually long metal sheets and beams with predefined cross-section.

A typical hot rolling mill consists of a,

- Heating furnace, for preparing the raw material to process

– Roughing mill, for obtaining a rough mid-product

– Finishing mill, for achieving desired quality

– Run-out-table, for cooling and transporting the end product

The roughing mill and the finishing mill consist of several cascaded tandem rolling stands. Each stand usually has two working rolls, two backup rolls, a hydraulic ram and a mill housing. The working rolls contact and thin the material; the backup rolls support the working rolls against the rolling force. The hydraulic ram is for controlling the rolling gap and the mill housing is to enclose the system.

The prominent factors that effects the thickness quality of the end-product can be listed as follows:

– Non-uniform temperature distribution,

– Quality and chemical composition of material

– Eccentricity of the rolls

– Speed of rolling

The inherent eccentricity of the rolls causes likewise periodic motions of mechanical cams, resulting in periodic thickness variations on the surface.

Due to impracticability of measuring the thickness of the formed sheet at the instant where the rolling process is happening, the sensor that has been placed away from the rolls causes a latency in the observation of system output. Therefore, a hot rolling mill in a whole can be considered to be a time-delayed system.

Additionally, due to the existence of hydraulic rams for arranging the roll gap, control of hot rolling mills are considered to be a type of systems with cascaded controllers: One controller must be designed for controlling the product thickness; this controller will evaluate the position of the rolls according to the calculated error in order to obtain desired thickness and surface properties. And another controller for the hydraulic ram, to successfully achieve the position commands given by first controller. The first mentioned controller can be considered to be the outer controller and the second can be considered to be the inner controller of the hot rolling mills.

This thesis is dedicated to an analysis of the outer controller for attenuating disturbance caused by eccentricity in a time-delayed hot rolling mill.

Also, since strong non-linearities are present in hydraulic rams, successful position control of hydraulic rams requires more advance strategies than linear control.

All the above stated facts makes the whole control design of hot rolling mill more complex and the solutions to it to be varied. Therefore, next section is dedicated to a survey of various techniques and solutions related to modeling and controlling of hot rolling mills proposed by academic community.

2 Survey of Literature

An analytic approach to derive the mathematical model of hot rolling mills was demonstrated in [2], [3] and [4] . The model of the mill was obtained by combining three mathematical models formed for three main dynamic structures and processes observed in the mills: mill stand, hydraulic system and rolling process. The mathematical model was later validated with measurements of the real mill and was stated to be quite accurate with real data. Such a derived model does not posses an explicit time-delay term because the information of thickness is obtained via calculation rather than measuring. However, formation of a mathematical model using analytical approach requires a careful study of parametric values and environmental conditions.

An alternative approach to obtain mathematical model is using measured input-output signals. For instance, in [5], a Finite Impulse Response (FIR) model of a rolling mill with three input and one output was obtained from the data generated by a stair-case experiment; the linear system approximation was done according to observations implying that the overall system behavior at operating points was linear. However, the system model obtained by this method is a discrete-time model. The benefits of having a continuous model over discrete model in identification was stated briefly in [6].

As mentioned earlier, hot rolling mills can be considered as time-delayed systems due to the latency in measuring system response. Hence, methods for approximating time-delay systems can be applied to form a data-driven model of the hot rolling mills[7]. A discrete-time model estimation, especially emphasizing on the estimation of input time-delay was discussed in [8]. In [9], continuous model identification was done by separately estimating parameters and time-delay. A filter-based approach for continuous system identification was used in [6]; a linear filter was applied to the input and output of the system, allowing, with further mathematical manipulation, the time delay term to be explicitly represented in parameter vector. An important advantage of the filter-based method is that it allows simultaneous identification of parameters and delay.

From the control point of view for hot rolling mills, different control methods were proposed to reject different types of disturbances. A controller design motivated by the idea of achieving desired thickness properties in the presence of temperature variations was discussed in [10]; a linear state-space representation of the rolling mill at its operating point was controlled with optimal control techniques. Methods of control for rejecting periodic surface variations caused by roll eccentricity was investigated in [11] and [12]. Both articles focus on the application of repetitive control method. A comprehensive explanation of repetitive control for rejecting periodic disturbance can be found in [13]. In [11], addition to repetitive controller, a μ-synthesis analysis was carried out to increase the overall robustness of the control system. In [12], application of multiple repetitive controller was studied in order to increase the variety of periodic disturbances that can be rejected.

For an introductory and comprehensive review of theory of systems and control the reader is referred to [14], [15] and [16].

3 System Identification

A *system* can be defined as any physical or ideal concept that takes an input, alters it and in return gives it back as an output. In some literature, the word *process* is used to refer to the word *system*, since both of the words refer to a change from one state to another.

Systems are classified with respect to their common properties. These classifications can be made according to their physical realization as well as to their mathematical description. Mathematically describing a system gives handful of methods to identify and analyze them. Also, thanks to mathematics, systems that look completely unrelated due to, for instance, being from different fields, can be represented by the same form of equations.

Systems can be described using different mathematical concepts such as differential equations, artificial neural networks, logic and etc. A wide range of physical and abstract phenomenon, for instance, engineering, biology and economy can be represented as a system. Here, in this thesis, systems that are expressed by linear time-invariant differential equations are going to be covered.

A system is called *linear* if it holds the superposition property:

Let $S\{\}$ denote a system that takes $x(t)$ as its input argument and gives $y(t)$ as its output i.e. $y(t) = S\{x(t)\}$. Then the superposition is defined as to hold the equation

$$\alpha y_1(t) + \beta y_2(t) = S\{\alpha x_1(t) + \beta x_2(t)\} \tag{1}$$

where α and β are scalars, and

$$\begin{aligned} y_1(t) &= S\{x_1(t)\} \\ y_2(t) &= S\{x_2(t)\} \end{aligned}$$

A new system can be formed by combining systems or an existing system can be explained as a combination of subsystems. The property of superposition brings a significant convenience to understand the resultant system when linear systems are combined. When dealing with complex systems like control systems, examining the system as a combination of subsystem brings a systematic approach to understand and improve the overall system.

A system is called *time-invariant* if its response characteristic does not change in time as expressed mathematically as,

$$S\{x(t)\} = y(t) \quad \rightarrow \quad S\{x(t - t_0)\} = y(t - t_0) \tag{2}$$

When a system holds the features denoted by Equation (1) and (2), the system is called a *linear time- invariant system.*

An important property of linear time-invariant systems is that if the impulse response of the system is known, the response of the system for any type of input signal can be evaluated. This property is represented by the integral

$$y(t) = \int_{-\infty}^{\infty} x(\tau)h(t - \tau)d\tau = x(t) * h(t) \tag{3}$$

This integral is called the *Convolution Integral* and what it basically does is that, it expresses the input signal $x(t)$ in terms of a infinite sum of impulses and applies the superposition principle to calculate the overall response by adding each of the individual impulse responses denoted by $h(t)$.

3.1 Signal Representation

In the field of signal and systems analysis, there exist two fundamental concepts to describe signals [14]:

- Signals expressed as a Sum of Impulses.
- Signals expressed as a Sum of Complex Exponentials.

As shown before, when a signal is expressed in terms of impulses, the convolution integral relates the input to output.

On the other hand, expressing signals as a combination of complex exponentials gives rise to powerful analysis tools like Fourier and Laplace transforms.

A complex exponential is defined simply as an exponential function having an imaginary term at its power such as,

$$x(t) = e^{(c_r + c_i j)t}$$

3.2 Fourier and Laplace Transform

Fourier Transform corresponds to a decomposition of signal in terms of a linear combination of complex exponentials [17]. However, it is possible to obtain the transformation directly by the use of Convolution Integral:

Let the input signal given to a system be $x(t) = e^{jwt}$. Then the output $y(t)$ can be found by the use of Convolution Integral :

$$\begin{aligned} y(t) &= \int_{-\infty}^{\infty} x(t-\tau)h(\tau)d\tau \\ &= \int_{-\infty}^{\infty} e^{jw(t-\tau)}h(\tau)d\tau \\ &= \left(\int_{-\infty}^{\infty} e^{-jw\tau}h(\tau)d\tau\right) e^{jwt} \\ &= \left(\int_{-\infty}^{\infty} e^{-jw\tau}h(\tau)d\tau\right) x(t) \end{aligned}$$

The integral,

$$H(jw) = \int_{-\infty}^{\infty} e^{-jwt}h(t)dt \tag{4}$$

corresponds to the Fourier Transform definition of the impulse response and it is denoted by $H(jw)$.

The integral in (4) represents the expression of a signal in terms of complex exponential $x(t) = e^{jwt}$; the result of this integral for a specific frequency w_s shows how much of the component $e^{jw_s t}$ has an influence in the signal.

The inverse of Fourier transformation is given by,

$$h(t) = \frac{1}{2\pi}\int_{-\infty}^{\infty} H(jw)e^{jwt}dt \tag{5}$$

and the convolution in time domain corresponds to multiplication in frequency-domain as,

$$y(t) = h(t) * x(t) \;\leftrightarrow\; Y(jw) = H(jw)X(jw) \tag{6}$$

In some cases, for instance, when a signal that does not converge to a certain value is tried to be expressed in terms of defined complex exponential used in Fourier Transform, the integral in (4) can not be carried out. To overcome this problem the complex exponential function definition in Fourier Transform is extended to have a variable not only with an imaginary part but also with a real part such as,

$$e^{(\sigma + jw)t}$$

Addition of the variable σ, allows the integral to converge at least for some values of σ. This new extended complex variable is called the Laplace variable and is denoted by s.

Simply exposing this extension to Fourier Transform results in what it is called the Laplace Transform:

$$H(s) = \int_{-\infty}^{\infty} e^{-st} h(t) dt \tag{7}$$

3.3 System Representation

Linear time-invariant systems with single input and single output (SISO) can be expressed by linear ordinary differential equation in the form of,

$$\begin{aligned}&\tfrac{d^n y}{dt^n} + a_1 \tfrac{d^{n-1} y}{dt^{n-1}} + ... + a_{n-2} \tfrac{dy}{dt} + a_{n-1} y(t) = \\ &= b_0 \tfrac{d^m x}{dt^m} + b_1 \tfrac{d^{m-1} x}{dt^{m-1}} + ... + b_{n-2} \tfrac{dx}{dt} + b_{n-1} x(t)\end{aligned} \tag{8}$$

A linear ordinary differential equation is basically an equation expressing the relationship between two signals in terms of their selves and their change.

The solution to a linear differential equation can be evaluated by examining the equation in its Laplace Transform. The use of Laplace Transform allows one to convert a problem of differential equation to a problem of algebraic equation. However, the solution obtained by solving the algebraic equation must be converted back using inverse Laplace transform in order to be valid for time-domain.

It is important to note that every linear system corresponds to a linear differential equation but not every linear differential equation corresponds to a linear system. If the differential equation has non-zero initial conditions, this prevents the superposition principle to be valid.

When the initial conditions are assumed to be zero, the Laplace Transform of Equation (8) is obtained as,

$$Y(s) = \frac{b_0 s^m + b_1 s^{m-1} + ... + b_{m-2} s + b_{m-1}}{s^n + a_1 s^{n-1} + ... + a_{n-2} s + a_{n-1}} X(s) \tag{9}$$

$$Y(s) = G(s) X(s) \tag{10}$$

where $G(s)$ is called the transfer function of the system. Notice that from Equation (6) and (10), it can be deduced that a transfer function of a system also corresponds to its impulse response.

If the system has an inherent time-delay [18], an exponential term is introduced to Equation (9) as

$$Y(s) = \frac{b_0 s^m + b_1 s^{m-1} + ... + b_{m-2} s + b_{m-1}}{s^n + a_1 s^{n-1} + ... + a_{n-2} s + a_{n-1}} e^{-\tau s} X(s) \qquad (11)$$

where τ is the time-delay between input and output. This exponential term comes from the Laplace Transform of shifted signals.

3.4 ARMAX Model of a System

ARMAX Model is a discrete time approximation of continuous models. The abbreviation ARMAX stands for Auto-Regressive Moving Average with Extra Input and the general form of an ARMAX model is given by the difference equation,

$$\begin{aligned} & y[k] = b_1 u[k-1] + b_2[k-2] + b_{n_b} u[k-n_b] - a_1 y[k-1] - \\ & -a_2 y[k-2] - ... a_{n_a} y[k-n_a] + e[k] + \\ & +c_1 e[k-1] + ... + c_{n_c} e[k-n_c] \end{aligned} \qquad (12)$$

where $y[k]$,$u[k]$ and $e[k]$ corresponds to discrete output, input and white noise signals, respectively. The number of terms for each signal is decided according to desired accuracy of the system; inclusion of more term will increase the continuous model order of the system that is been identified. The unknown coefficients are obtained by using least square method [19],[20], [21].

4 Stability Analysis

4.1 Stability as a System Property

Stability of a system is a property that expresses the behavior of a system under given inputs and it forms the primary goal for a controller to achieve. A system is called *stable* if the output remains bounded when it is subjected to a bounded input. For linear systems as represented by Equation (11), stability is a property of the system; in other words, the property of stability is independent from the type of input and initial conditions. However, for nonlinear systems, this fact is not true and stability of the system can depend on the type of input and initial conditions.

The reason why stability has different characteristics in linear and nonlinear systems can be explained by the concept of singular points of a system.[22]. When a system is expressed in its state-space representation, singular points are the states in the state-space where no change of its states occur; when a system starts at a singular point it will stay at rest. A system can basically behave in three manners when initiated around a singular point: it can either converge to the singular point, or diverge from the singular point or have a limit cycle around the singular point. In the classical stability terms they correspond to stable, unstable and marginally stable behavior, respectively. Linear systems have only one singular points due to having only one solution for the set of linear equations and the stability characteristics around this singular point is certain. Nevertheless, nonlinear systems can have multiple singular points and each can be particularly stable or unstable. Since in this thesis, linearity of systems are assumed, stability is accepted as a system property and the following section are devoted to the analysis of it.

4.2 Stability of Linear Systems

As mentioned previously, linear systems can be represented by transfer functions which are just ratios of polynomials. The values of s that make the transfer function equal to zero are called the zeros of the system and similarly, the values that make the transfer function approach to infinity are called poles. The polynomial at the denominator is also called the characteristic equation of the system and the signs of its roots decide whether the system is stable or unstable. Note that the roots of the characteristic equation correspond to the poles of the system. If the roots of the characteristic equation all have minus sign then the system is stable. If at least one of the roots has positive sign, it is unstable.

This fact can be made clear via first understanding the Laplace Transform of a real exponential function and then representing a transfer function in terms of partial fractions.

Laplace transform of a time-domain real exponential function $x(t) = e^{-\alpha t}$ can be found by using directly the definition of Laplace Transformation:

$$\begin{aligned}
X(s) &= \int_0^\infty e^{-\alpha t} e^{-st} dt \\
X(s) &= \int_0^\infty e^{-(\alpha+s)t} dt \\
X(s) &= \frac{1}{s+\alpha} e^{-(\alpha+s)t} \mid_0^\infty \\
X(s) &= \frac{1}{s+\alpha}
\end{aligned}$$

As it can be seen, the Laplace Transform of a real exponential function is a simple fractional function. Notice that when α is positive the exponential function converges to zero and when α is negative it goes to infinity as time passes.

A transfer function can be expressed in terms of a combination of fractional functions similar to that of the Laplace transform of the time-domain exponential function. This is done via applying partial fraction decomposition.

Let the transfer function be expressible by the ratio of two polynomials $N(s)$ and $D(s)$ such as,

$$G(s) = \frac{N(s)}{D(s)}$$

and assume that the denominator $D(s)$ has distinct roots $p_1, p_2, p_3, ...p_n$ that allow it to be expressed as

$$D(s) = (s + p_1)(s + p_2)(s + p_3)...(s + p_n)$$

then the transfer function $G(s)$ can be expressed as a combination of simpler transfer functions as,

$$G(s) = \frac{N(s)}{D(s)} = \frac{A}{(s+p_1)} + \frac{B}{(s+p_2)} + \frac{C}{(s+p_3)} + ... + \frac{D}{(s+p_n)} \quad (13)$$

where A, B, C and D are polynomials that satisfies the equality.

Using the information obtained from the Laplace transform of the exponential function, one can conclude that if any of the partial fraction terms have a p_i with a negative value, it will cause a divergence towards infinity and will result into an unstable behavior in total response even though other terms converge to zero.

If the transfer function of a system has a pole with a positive real part or in other words, has a pole that is located in the right hand-side of the s-plane, then the system is unstable. Similarly, if all of the poles are located in the left hand-side of the s-plane then the system is stable.

Hence, when analyzing the stability of a linear system, evaluation of the pole's locations are sufficient to make a decision on the system stability.

4.3 Argument Principle

A complex function $F(s)$, like a system transfer function, will have values that form a set corresponding to a closed-contour in the plane of the dependent variable $F(s)$, when the independent complex variable s tracks a closed-contour in its own s-plane.

Cauchy's argument principle relates the number of encirclement around origin in the $F(s)$ plane, to the number of zeros and poles of the complex function $F(s)$ that are present inside the contour that has been tracked in s-plane [23].

When a complex function $F(s)$ is mapped to $F(s)$ plane via tracking in a clockwise direction a continuous closed contour in the s-plane which does not pass through any zeros or poles, the principle's conclusions can be listed as follows :

- If the contour in the s-plane encloses a pole of $F(s)$, there is one encirclement of the origin of the $F(s)$ plane in the counterclockwise direction.
- If the contour in the s-plane encloses a zero, there is one encirclement of the origin of the $F(s)$ plane in the clockwise direction.
- If the contour in the s-plane encloses same number of zero and poles or does not enclose any zero and pole at all, there is no encirclement around the origin of the $F(s)$ plane.

The above conclusion can be expressed in an equation simply as,

$$N = Z - P \tag{14}$$

where N is the number of clockwise direction around the origin and Z and P are the number of zeros and poles the contour encloses, respectively.

4.4 Polar Ploting

Polar plot of a system is a graphical representation of its frequency response. Instead of reviewing the magnitude and phase change separately as done in Bode plot, polar plot shows the information of both magnitude and phase characteristics in one complex-plane [15].

Polar plot of a system is obtained by simply inserting s values that varies from $0i$ to $+\infty i$ to the systems' transfer function and then plotting the resulting complex numbers in the complex plane. When a polar plot is formed by swiping the complex variable s from $-\infty i$ to $+\infty i$, a graph what it is called the Nyquist plot is formed.

When the polar plot is plotted from minus infinity to infinity, it forms a loop. This is due to the fact that the frequency response for negative frequencies is just the mirror image of the frequency response of the positive frequencies with respect to real-axis. By plotting the graph from minus infinity and infinity, these two symmetrical responses will be plotted together and form a loop. This loop holds an important part of the stability analysis when using Nyquist stability criteria.

4.5 Nyquist Stability Criterion

The Nyquist stability criterion encompasses the argument principle to investigate the stability of a system by checking the availability of poles in the right hand-side of the s-plane. The main idea of the criteria is to check the number of encirclements around the origin when the contour that has been tracked comprises all the right hand-side. This contour is called the Nyquist contour and can be imagined as a semi circle with a infinite radius that covers all the right hand-side of the s-plane. Choosing the contour in this manner guarantees to enclose all the positive zeros and poles that the system has and results in a Nyquist plot.

One important convenience that the Nyquisit stability criteria brings is that the stability of a closed-loop system can be investigated directly from its open-loop transfer function.

Suppose a system has a negative feedback structure with a open-loop transfer function expressed as,

$$G_{open} = C(s)G(s)$$

Then the closed-loop transfer function will have the form of,

$$G_{closed} = \frac{C(s)G(s)}{1 + C(s)G(s)} = \frac{G_{open}}{1 + G_{open}} \tag{15}$$

To guarantee that the closed-loop is stable, the closed-loop transfer function must have no poles on the right-hand side which means in other words, that the transfer function at the denominator $1 + C(s)G(s)$, must not have any zeros at the right hand-side.

When a transfer function F(s) is summed with a positive number as in the denominator of the closed-loop transfer function, this results just in a shift towards the positive-side on the real-axis in the F(s) plane. So when investigating the number of encirclements around the origin of a transfer function in the form of $n + F(s)$, the information can be obtained by checking the number of encirclements around the point $-n + 0i$ of the transfer function $F(s)$ in their own corresponding planes.

Hence the argument principle can be modified to what it is called as the Nyquist stability criteria, to analyze the stability of the closed-loop system directly by examining the open-loop transfer function $C(s)G(s)$:

Let Z' and P' denote the number of zeros and poles of the transfer function $1 + C(s)G(s)$ and N' to denote the number of encirclements around $-1 + 0i$ in the Nyquist plotting of $C(s)G(s)$, then argument principle relates them, as shown before, as

$$N' = Z' - P'$$

Using this modified argument principle, the Nyquist stability criteria can be stated as follows:

To achieve closed-loop system stability the relation $N' = -P'$ must be satisfied, since in a stable closed-loop system $Z' = 0$ [24].

5 Internal Model Control

Internal Model Control method or for short IMC can be reviewed as a different interpretation of the classical control method. This interpretation emphasizes on how the real system response deviates from the expected response.

The idea of internal model control made its official first mark in 1976 in the work of B.A. Francis and M. Wohnam [25] and later on developed to cover many control problems by succeeding engineers.

In classical feedback control, the response of the controlled system and the reference value is continuously compared to generate an error. Then according to the error, the controller decides and takes an action to minimize this error. However, when the error is calculated by directly subtracting the system response from the reference signal for a given instant, a loss of information occurs. This lost information corresponds to the knowledge of source which causes the difference between the reference value and real system response. The source of error could be due to change of reference value, a improper choice of controller, pure response characteristics of the system, internal or external disturbances and etc.

To clarify the cause of error and to design a controller with respect to it, the classical feedback control is rearranged to have a form that is now named as internal model control. In this control strategy, the error is calculated in two steps. In the first step, the real response of the system and expected system response are compared. Both of the responses are obtained for the same type of reference. If the real system and its model is well consistent, the first comparison reveals mainly the presence of external disturbance. However, it does not have to

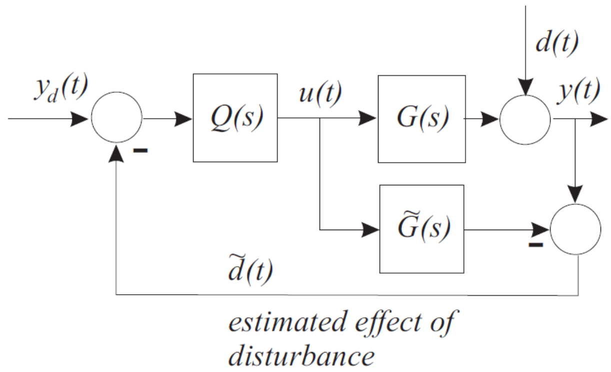

Figure 1: Block Diagram of Internal Model Control [1]

necessarily correspond to an external disturbance only; the difference can also occur due to input disturbance or inconsistent plant model. Then in the second step, the result of the first step is compared with the reference signal. The result of the second comparison corresponds to the error which is interpreted by the controller to generate a control action aiming to minimize the error.

As it is explained, the principle control idea of internal model control is almost the same with the classical feedback control. The only main difference is that due to the error generation of IMC reveals the external disturbance more clearly, the controller can be designed to deal with disturbances effectively. As it will be explained later, if the type of disturbance is known, the controller can be improved by adding a component that cancels the disturbance. Straightforwardly, if the controller has the structure of the disturbance in itself, it can use this structure to cancel the disturbance by sending the negated form to the it.

A typical internal model control system has a block diagram as shown in Figure 1 [26]. Here $Q(s)$, $G(s)$ and $\widetilde{G}(s)$ denote the transfer functions of the controller, plant and its model, respectively. The closed-loop transfer function is obtained as in the following manner:

$$Y(s) = D(s) + G(s).U(s) \tag{16}$$

$$U(s) = Q(s)\epsilon(s) \tag{17}$$

$$\epsilon(s) = Y_d(s) - \left(Y(s) - \tilde{G}(s)U(s)\right) \tag{18}$$

$$U(s) = Q(s)Y_d(s) - Q(s)Y(s) + Q(s)\tilde{G}(s)U(s) \tag{19}$$

Substituting Equation (19) to (16) results in:

$$Y(s) = D(s) + G(s)\frac{Q(s)Y_d(s) - Q(s)Y(s)}{1 - \left(Q(s)\tilde{G}(s)\right)}$$

$$Y(s)\left(1 - Q(s)\tilde{G}_s\right) = G(s)Q(s)Y_d(s) + \left(1 - Q(s)\tilde{G}(s)\right)D(s) - G(s)Q(s)Y(s)$$

$$Y(s)\left(1 - Q(s)\tilde{G}(s) + G(s)Q(s)\right) = D(s)\left(1 - Q(s)\tilde{G}(s)\right) + G(s)Q(s)Y_d(s)$$

$$Y(s)\left(1 + Q(s)\left(G(s) - \tilde{G}(s)\right)\right) = G(s)Q(s)Y_d(s) + \left(1 - Q(s)\tilde{G}(s)\right)D(s)$$

$$\boxed{Y(s) = \frac{GQ}{1 + Q\left(G - \widetilde{G}\right)}Y_d(s) + \frac{1 - \widetilde{G}Q}{1 + Q\left(G - \widetilde{G}\right)}D(s)} \tag{20}$$

If the plant and its model are assumed to be completely consistent with each other such that $G(s) = \tilde{G}(s)$, further simplification of the close-loop transfer function shown in Equation (20) can be made:

$$\boxed{Y(s) = GQY_d(s) + (1 - \widetilde{G}Q)D(s)} \tag{21}$$

5.1 Conversion between Classical Feedback Control and Internal Model Control

It is possible to convert a classical feedback control into a representation of internal model control and vice versa. The relationship between IMC version and classical version of a controller can be found by equating the transfer functions of both closed-loop systems [1].

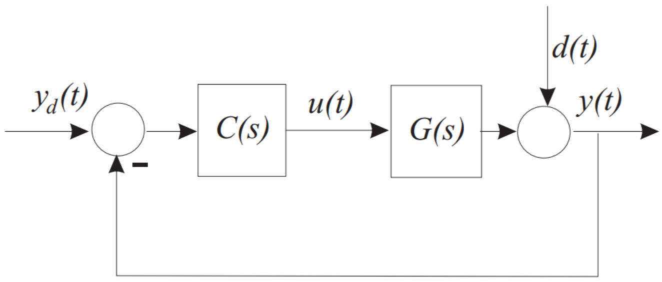

Figure 2: Block Diagram of Classical Feedback Control [1]

The closed-loop transfer function for a typical classical feedback control system as depicted in Figure 2 is given by,

$$Y(s) = \frac{C(s)G(s)}{1 + C(s)G(s)}Y_d(s) + \frac{1}{1 + C(s)G(s)}D(s) \tag{22}$$

Since Equation (20) and (22) represents the same physical system, the transfer functions between output and inputs must be equal:

$$\frac{C(s)G(s)}{1+C(s)G(s)} = \frac{G(s)Q(s)}{1+Q(s)\left(G(s)-\tilde{G}(s)\right)} \tag{23}$$

$$\frac{1}{1+C(s)G(s)} = \frac{1-\tilde{G}(s)Q(s)}{1+Q(s)\left(G(s)-\tilde{G}(s)\right)} \tag{24}$$

By picking any of Equation (23) and (24), the expression of $C(s)$ in terms of $Q(s)$ can be obtained with further mathematical manipulation:

$$\begin{aligned} C(s)+Q(s)C(s)\left(G(s)-\tilde{G}(s)\right) &= Q(s)+C(s)G(s)Q(s) \\ C(s)-Q(s)C(s)\tilde{G}(s) &= Q(s) \\ C(s)\left(1-Q(s)\tilde{G}(s)\right) &= Q(s) \end{aligned}$$

$$\boxed{C(s) = \frac{Q(s)}{1-Q(s)\tilde{G}(s)}} \tag{25}$$

Using Equation (25), an important concept of disturbance rejection can be shown. Let the physical control system hold the simplification covered by Equation (21) and let the classical representation of the controller contain the model of the disturbance such that,

$$C(s) = A(s)D(s) \tag{26}$$

where A(s) represents the rest of the controller such that $A(s) \neq 0$.

Substituting this classical controller model into Equation (25) yields,

$$A(s)D(s)\left(1 - Q(s)\tilde{G}(s)\right) = Q(s) \tag{27}$$

Now if the IMC Controller is stable in way that

$$\lim_{s \to 0} sQ(s) = 0$$

in steady state, Equation (27) becomes equal to zero. Since A(s) is non-zero, this means that $(1 - Q(s)\tilde{G}(s))D(s)$ must be zero. Notice that this term corresponds to the transfer function between output and disturbance in Equation (21). When this term converges to zero, it guarantees asymptotic disturbance rejection.

The conclusion of the above explanation is that in order to be able to attenuate disturbance completely, the classical controller C(s) must contain the model of the disturbance.

Having the mathematical description of Internal Model Control method at disposal allows one to design the controller more effectively if disturbance is wanted to be attenuated.

5.2 Repetitive Control

If the disturbance that is desired to be rejected is a periodic signal, a sub-field of IMC method, called Repetitive Control technique can be used to design the controller. The Repetitive Control method can be derived directly from the Internal Model Control, however, due to its success in rejecting this particular disturbances by making small modification to the IMC and interpreting it from a different point of view, this method is considered to be a standalone control technique

[27], [28].

In this thesis, the conditions needed to be satisfied to reject periodic disturbance, are going to be derived from the Internal Model Control. This derivation process will also reveal the fundamental idea underlying Repetitive Control.

As mentioned earlier, from Equation (21), conditions needed to be satisfied by the controller can be derived for disturbance rejection:

$$\begin{aligned} \left(1 - \tilde{G}Q\right) D(s) &= 0 \\ D(s) - \tilde{G}QD(s) &= 0 \end{aligned}$$

If the term $\tilde{G}Q$ can be made equal to one, the disturbance will cancel itself, resulting in the rejection of disturbance. The key idea here is now to find such a controller $Q(s)$ to achieve this fact.

The first statement that can be made is that if the controller posses the inverse of model $\tilde{G}$ such that

$$Q(s) = \frac{1}{\tilde{G}} R(s) \tag{28}$$

where R(s) denotes the rest of the controllers transfer function, the effect of the plant can be removed. What it is ended up with, after this controller model is inserted for $Q(s)$, is,

$$\tilde{G}Q(s) = R(s)$$

Hence, the controller $Q(s)$ should posses the inverse of the model.

The second statement concerns the controllers rest part $R(s)$. This part of the controller must be designed such that the equality,

$$D(s)R(s) = D(s)$$

must be valid. This means nothing but $R(s)$ should have the properties,

$$|R(s)| = 1 \quad (29)$$

$$arg\,(R(s)) = 2k\pi, \quad k = 0, \pm 1, \pm 2, ... \quad (30)$$

Any periodic disturbance can be thought of as a finite signal being repetitively added to itself after a time delay equal to the time length of the original signal. This can be mathematical expressed in the following manner: Let $P(s)$ denote a finite signal corresponding to one period of the periodic signal and T_p to be the time length of the signal $p(t)$ or, in other words, the period of the periodic signal. Then, the periodic signal can be expressed as,

$$Y(s) = \frac{1}{1 - e^{-T_p s}} P(s) \quad (31)$$

Using Equation (31) any periodic disturbance can be modeled and implemented into a controller. Since the controller contains a disturbance model generated by repetitive addition, it is called Repetitive Controller.

However, for the sake of simplicity, from now on, the periodic disturbance is going to be assumed and modeled as it is a sinusoidal signal such as,

$$d(t) = A_d sin(w_d t) \tag{32}$$

The consequence of having a sinusoidal disturbance is that Equation (29) and (30) can be simplified to,

$$\begin{aligned} |R(jw_d)| &= 1 & (33) \\ arg\,(R(jw_d)) &= 2k\pi, \quad k = 0, \pm 1, \pm 2, ... & (34) \end{aligned}$$

Equation (28), (29) and (30) are the requirements to form the controller $Q(s)$ to reject disturbance from the system response. Additionally, it is also desired to have the controller to achieve reference tracking , for instance, for a unit step reference signal. For this purpose, the limit which refers to the final value theorem applied to the step response,

$$\lim_{s \to 0} sG(s)Q(s)\frac{1}{s} = \lim_{s \to 0} R(s) = 1 \tag{35}$$

must be satisfied.

To satisfy Equation (33), (34) and (35), a transfer function of the form

$$R(s) = F(s)e^{-\theta s} \tag{36}$$

can be used. Here, $F(s)$ represents a stable filter having a unit step gain equal to one and $e^{-\theta s}$ represents a user-definable time delay to allow the controller to satisfy Equation (34).

Finally, by combining all of the discussed properties needed to be satisfied by the controller for a proper control, the IMC controller has a form of,

$$\boxed{Q(s) = \frac{1}{\tilde{G}}F(s)e^{-\theta s}} \tag{37}$$

and holds the following conditions:

$$\boxed{\begin{aligned} |F(jw_d)| &= 1 \\ arg\,(F(jw_d)) - w_d\theta &= 2k\pi, \quad k = 0, \pm1, \pm2, ... \end{aligned}} \tag{38}$$

5.3 Robustness

Robustness of a controller is an important property that must be taken into account when the controller is desired to be implemented on a real system. Robustness of a controller is the measure of the quality of how far a controller will carry out a successful control when there are differences present in the nominal parameter values or unexpected system conditions like disturbance. The more robust the controller is, the more it will be immune to environmental changes and design errors.

There exist many techniques to measure and improve the robustness of a controller such as gain/phase margin analysis and H_∞ optimization [29].

Gain/phase margin analysis is a simple method to make comments on robustness when two controller are compared. However, it does not give direct implications to the information of the point at which the controller starts to fail. For this purposes, more advanced analysis techniques must be used.

Gain margin is a property of the system which indicates how much of a gain increase leads to system instability. It can have either a positive or a negative value. A positive gain margin implies that a certain amount of gain increase will make the system to lose its stability; a negative gain margin implies that a certain amount of gain reduction will cause instability.

Phase margin is the property which tells about how much of a phase shift in the overall system can cause unstable behavior.

In terms of gain/phase margins, robustness of the controller increases as the value of the margins increase. Gain/phase margin is obtained by first deriving the frequency response of the open-loop control system either in Nyquist plot or in polar plot or in Bode plot.

The open-loop control system transfer function of IMC can be easily obtained using the relationship between IMC and Classical Feedback Control. It is known that the open-loop transfer function of Classical Feedback Control is,

$$G_{openloop}(s) = C(s)G(s)$$

Substituting the derived equation for relation between classical controller $C(s)$ and IMC controller $Q(s)$, and assuming $G(s) = \tilde{G}(s)$, the open-loop transfer function for IMC is obtained as,

$$IMC_{openloop}(s) = \frac{F(s)e^{-s\theta}}{1 - F(s)e^{-s\theta}} \tag{39}$$

Once the open-loop transfer function is obtained, the gain and phase margin can be obtained by using MATLABs built-in function `margin` or with a self-written code.

When a system is known to be stable, polar plotting can be used to evaluate the gain and phase margins of the system. By finding the intersection points between the curve and the negative real axis, and then choosing the furthest one from the origin, the necessary information can be obtained for the calculation of gain margin. Additionally, the necessary information for phase margin can be found by finding the intersection points between the curve and the unit circle. The point which is the closest to the negative real axis is used to calculate the phase margin.

A system can have multiple values of gain and phase margins with different signs and values. This fact causes the system stability to be upper and lower bounded in terms of gains and phase shifts which leads to a concept called as conditional stability. An internal model control system as introduced in this thesis can have multiple gains/phase margins and in the analysis of robustness of this type of systems, the lowest positive gain margin value among all evaluated gain margins will be the gain margin to be taken into account. In this thesis, robustness analysis with respect phase margin will not be emphasized much due to imprecision of numerically calculating the margin itself.

5.4 Application of Repetitive Control to Time-Delay Systems

As discussed earlier, a system with time-delay τ has an exponential term in its transfer function. This fact causes a need for a small modification to the form of IMC controller in Equation (37), conditions introduced for filter in Equation (38) and open-loop transfer function in Equation (39).

If a system $S(s)$ has a transfer function expressed in

$$S(s) = G(s)e^{-s\tau}$$

where here $G(s)$ corresponds to the part of $S(s)$ without time-delay and $e^{-s\tau}$ is the time-delay component of $S(s)$, then Equation(37), (38) and (39) are modified to explicitly cover time-delay systems as,

$$\boxed{Q(s) = \frac{1}{G(s)} F(s)e^{-(\theta+\tau)s}} \tag{40}$$

$$\boxed{\begin{array}{rcl} |F(jw_d)| & = & 1 \\ arg\left(F(jw_d)\right) - w_d(\theta+\tau) & = & 2k\pi, \quad k = 0, \pm 1, \pm 2, ... \end{array}} \tag{41}$$

$$\boxed{IMC_{openloop}(s) = \frac{F(s)e^{-s(\theta+\tau)}}{1 - F(s)e^{-s(\theta+\tau)}}} \tag{42}$$

The stability condition of the repetitive control system can be evaluated by directly checking the poles of its closed loop transfer function. Using Equations (15) and (42) the closed-loop transfer function can be found as,

$$\begin{aligned} IMC_{closedloop}(s) &= \frac{F(s)e^{-s(\theta+\tau)}}{1 + F(s)e^{-s(\theta+\tau)} - F(s)e^{-s(\theta+\tau)}} && (43) \\ &= F(s)e^{-s(\theta+\tau)} && (44) \end{aligned}$$

Equation (44) implies that as long as a stable filter is used and the assumptions are valid, the repetitive control will be stable.

6 Objectives

The topic this thesis covers was also investigated in the past in [30]. Hence, this thesis aims to bring improvement and convenience to the application of repetitive controller to hot rolling mills that was once investigated.

The objective of this thesis, by being strict to the theoretical knowledge mentioned above, is to extend the scope of study of previous works and to achieve,

1. Development of an algorithm to obtain time-delay system models of hot rolling mills from experimental data
2. A model of filter that increases the robustness of repetitive controller in internal model control system
3. Development of an algorithm that tunes the filter for the given conditions like disturbance and time-delay present in the system.

Part II

Applications

7 System Evaluation using Data

First-order systems with time-delay provide simple yet effective approximations of systems with high-order. Since they have only three parameters to be evaluated, the optimization of approximating higher order systems or system identification from measured data is fairly less complicated and fast. However, important informations like pole/zero locations, high frequency characteristics of the real system are lost.

In accordance with Equation (11), a first-order system with time-delay has a transfer function in a form of,

$$G(s) = \frac{K}{Ts+1}e^{-\tau s} \tag{45}$$

For the given measurement of the hot rolling mills input and output as shown in Figure 3 the introduced algorithm in this thesis for estimating a first order system with time-delay follows the steps as listed:

1. Preparation of the Measured Data for Identification via Normalization
2. Estimation of Overall Time-Delay using Cross Correlation
3. Shifting Output Data from left to right to find the best fitting ARMAX Model

4. Conversion of ARMAX Model to Continuous-time model
5. Calculation of Time-Delay by adding the Corresponding Shift in Step 3 to Overall Delay calculated in Step 1.

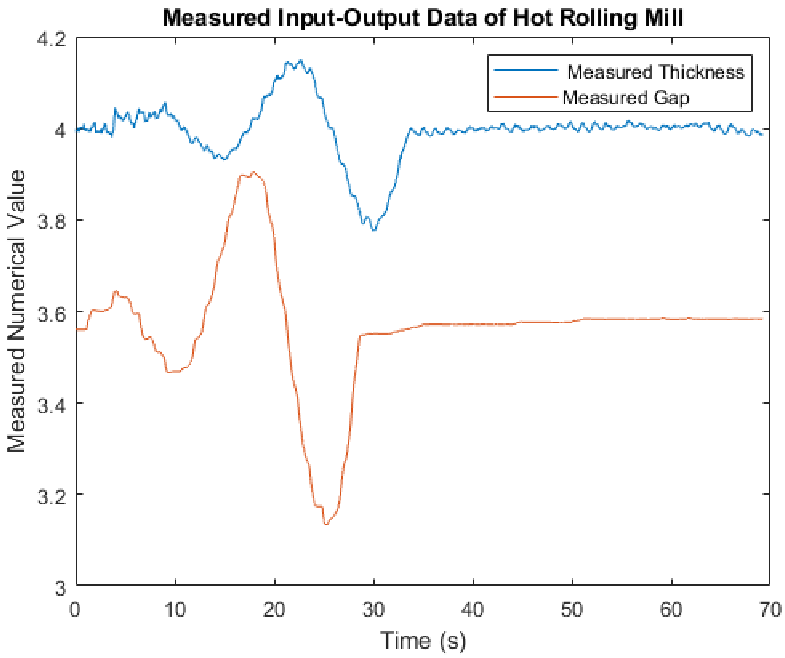

Figure 3: Measured Input-Output Data of Hot Rolling Mill

7.1 Step 1 - Normalization of Data

The input $u(t)$ and output $y(t)$ signals are normalized by subtracting each signals mean value from the signals itselves:

$$y_{normalized}(t) = y(t) - mean\,(y(t))$$
$$u_{normalized}(t) = u(t) - mean\,(u(t))$$

The normalized input and output signals can be seen in Figure 4.

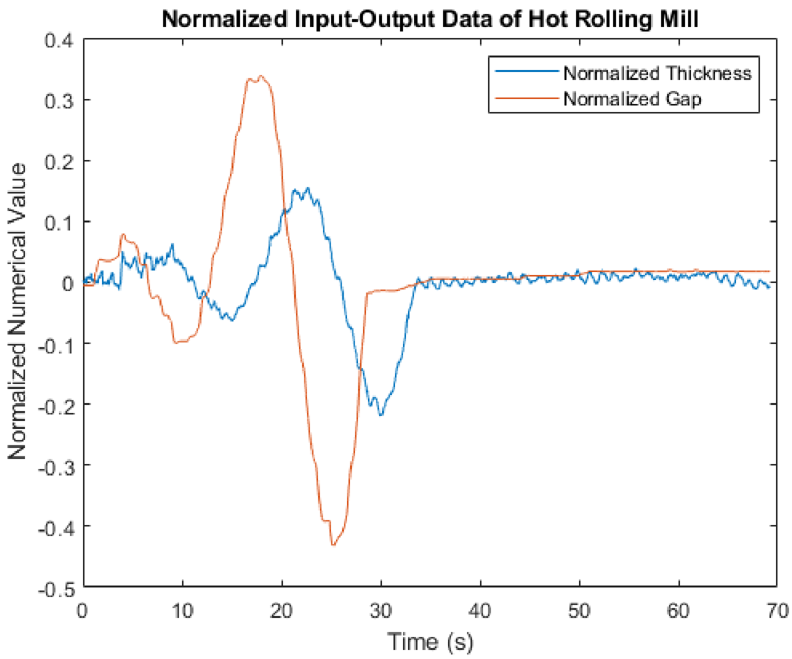

Figure 4: Normalized Input-Output Data of Hot Rolling Mill

7.2 Step 2 - Estimation of Overall Delay

Cross-correlation is a mathematical tool for examining the linear dependency between two signals. By swiping one signal over the other, the effect of shifting between signals on linear dependency can be found as shown in the Figure 5. Cross-correlation coefficient is the normalization of cross-correlation and it is a scale for linear dependency. When the cross-correlation coefficient is 1 or -1 it means that for the given shift between signals, there is a perfect positive or a negative linear dependency between signals, respectively. If the coefficient is zero, it means that there is no linear dependency.

Using cross-correlation between input and output for estimating the time-delay of single-input-single-output systems is an effective method. Since first-order system model is used for the estimation, it is expected to have a high linear dependency between input and output. The corresponding time-shift for maximum cross-correlation coefficient corresponds to the overall delay of the system [31].

The overall time-delay consists the information of time-delay τ and the time constant T of the system. Therefore, further operations must be carried out to evaluate these two parameters from the overall time-delay.

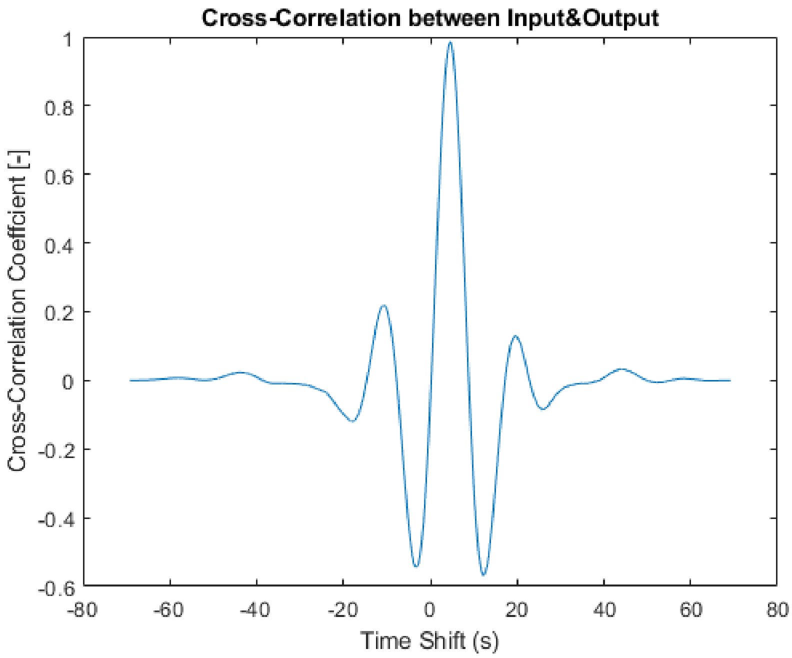

Figure 5: Cross Correlation between Normalized Input-Output

From Figure 5, the overall delay is found as 4.6250 seconds.

7.3 Step 3 - Estimation of Time Constant T and Unit-step Gain K

By taking the overall time-delay as a reference for how much of a shift of time is needed to cancel the effect of time-delay τ, a first order model is fitted to the new shifted data using Auto-Regressive Moving-Average Extra-Input (ARMAX) system model. Since it is not known exactly how much of a time-delay is present in the system, a series of ARMAX model estimation is carried out for various values of time-delay in a close range to overall time-delay. Each generated ARMAX model is compared with the real measurements and the one with least error is picked to be the best approximation of the real system.

The result of such an ARMAX model estimation for a given relative time shift with respect to overall time delay can be seen in Figure 6. Relative time-shift is defined as the amount of increment or decrement to the overall time-delay. The minus sign in relative time shift represents a decrement of overall time-delay. The summation of overall time delay and relative time shift gives the time-delay τ used for estimating parameters K and T.

As it can be seen, when the system has a relative time-shift of -0.1 seconds, the ARMAX Model with least error is achieved.

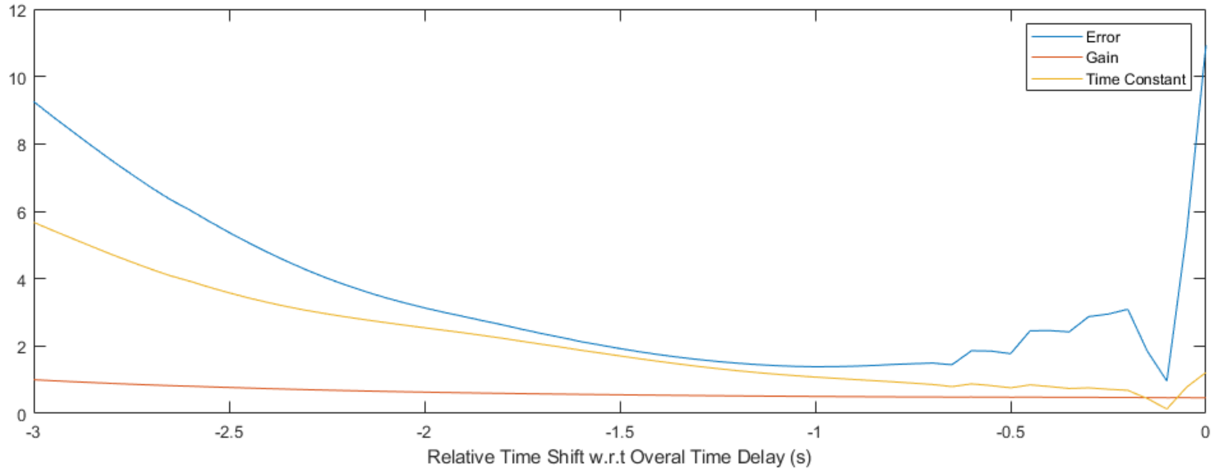

Figure 6: System Parameter Value and Estimation Error for given Relative Time-shift

7.4 Step 4 - Conversion of ARMAX Model to Continuous-time Model

Since ARMAX Model is a discrete-time model, it needs to be converted to continuous time model to have a representation of Equation (12). This conversion is made by using the built-in function in MATLAB [32]:

```
continuous_model = d2c(discrete_model)
```

As default, the function `d2c` uses zero-order hold method to convert discrete-time model to continuous-time model. The obtained continuous model via this function is,

$$G(s) = \frac{3.534}{s + 7.561}$$

7.5 Step 5 - Calculation of Time-Delay τ

The overall delay and the relative time-shift was found as 4.6250s and -0.1s, respectively. The time-delay of the system is calculated by adding these two values:

$$\tau = 4.6250 + (-0.1) = 4.5250s$$

The resultant system model for the given measured data after following the described algorithm is found as,

$$\boxed{G(s) = \frac{3.534}{s + 7.561} e^{-4.5250s}} \tag{46}$$

Figure 7 shows the time response of the obtained model with the real measured output for the measured input data.

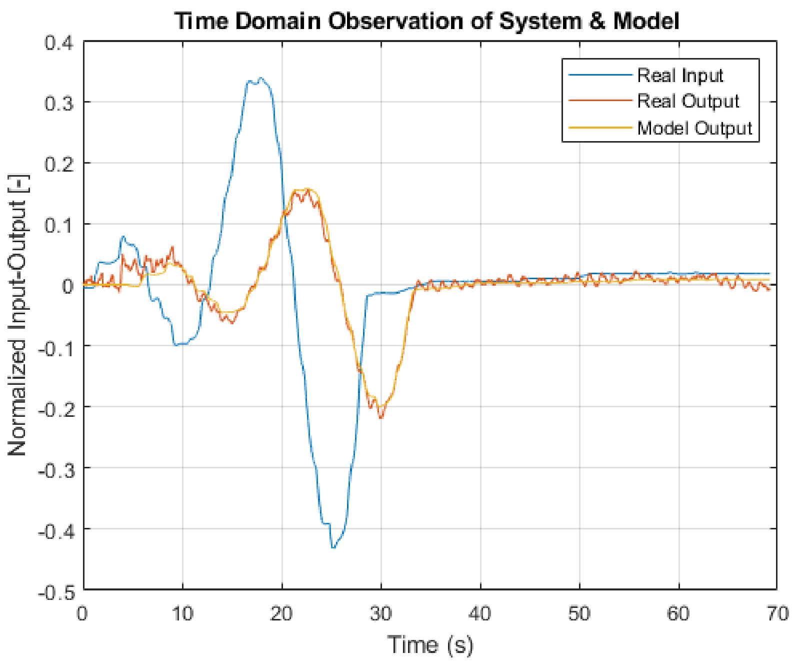

Figure 7: Time Response of Real System and Model subjected to Measured Input Signal

8 Disturbance Model

After evaluation of the system model, the disturbance signal can be obtained by subtracting the model output from real output as,

$$d(t) = y(t) - \tilde{y}(t)$$

In Figure 9, the real disturbance acting on the system is depicted by the blue line. To capture the characteristic repetition observed in the real disturbance, fast Fourier transform is applied to decompose the signal into its harmonic components. Figure 8 shows the frequency spectrum of the disturbance.

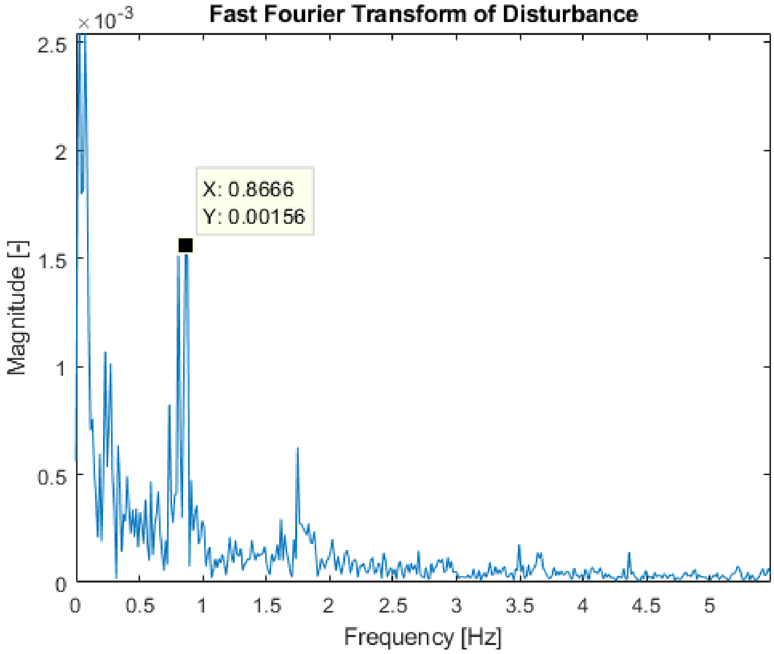

Figure 8: Fast Fourier Transform of Disturbance

According to Figure 8 harmonic components with lowest frequencies form the structure of the disturbance signal. However, the information of the prominently observed oscillation is obtained in the next most effective harmonic components pointed in the figure.

Using just this pointed component, a sinusoidal signal simplification of the disturbance can be formed as,

$$\boxed{d(t) = 0.00156 sin(2\pi\ 0.8666\ t)} \tag{47}$$

The obtained simple disturbance model is also plotted in Figure 9 and it can be seen that the information of the dominant oscillation frequency is captured.

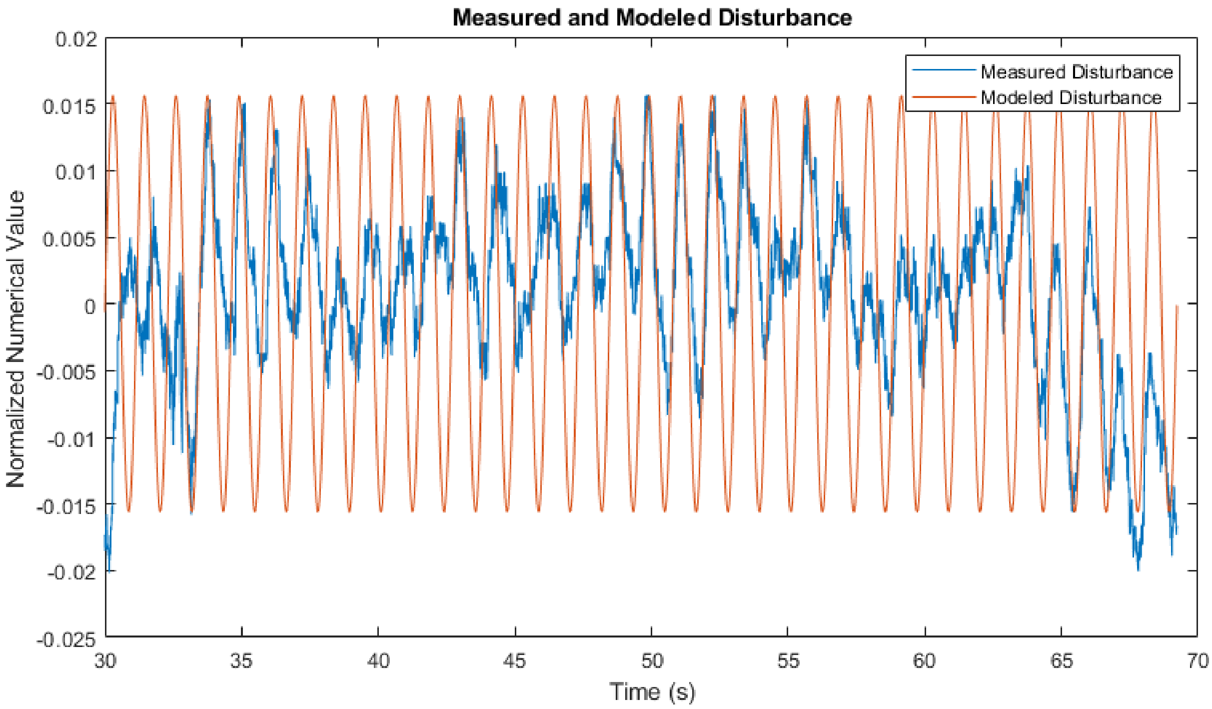

Figure 9: Measured and Modeled Disturbance

9 Filter Design for IMC Controller

The purpose of this section is to introduce a method to derive a filter having the features needed for attenuating a periodic disturbance in a repetitive control system.

In a simplified repetitive control system, the relationship between output and the inputs can be expressed by,

$$Y(s) = GQY_d(s) + (1 - \widetilde{G}Q)D(s) \tag{48}$$

Here G and $\widetilde{G}$ denotes the actual plant and its model, respectively; for the sake of simplicity, the plant and plant model is assumed to be identical. The controller Q must be designed in such a way that disturbance signal $D(s)$ must be rejected as much as possible whilst the system tracks the reference signal $Y_d(s)$.

As it is concluded by Equation (48), the controller can satisfy the above design criteria when it has the form of,

$$Q(s) = \frac{1}{G}F(s)e^{-\theta s} \tag{49}$$

The filter $F(s)$ is used to assure proper unit step response and a frequency response such that it causes the term $(\widetilde{G}Q)$ to have a gain of unity at the frequency of disturbance which means that the first-order filters are not-suitable for the solution and at least a filter with order of two must be used. The user-definable time-delay component is introduced to guarantee a phase-shift equal to the multiples of 360 degrees.

When the controller $Q(s)$ has the form of Equation (49) with appropriate parametric values, the disturbance D(s) automatically cancels itself.

Hence, from the above discussion and for good robustness, the filter should have a form of magnitude vs frequency response as depicted in Figure 10.

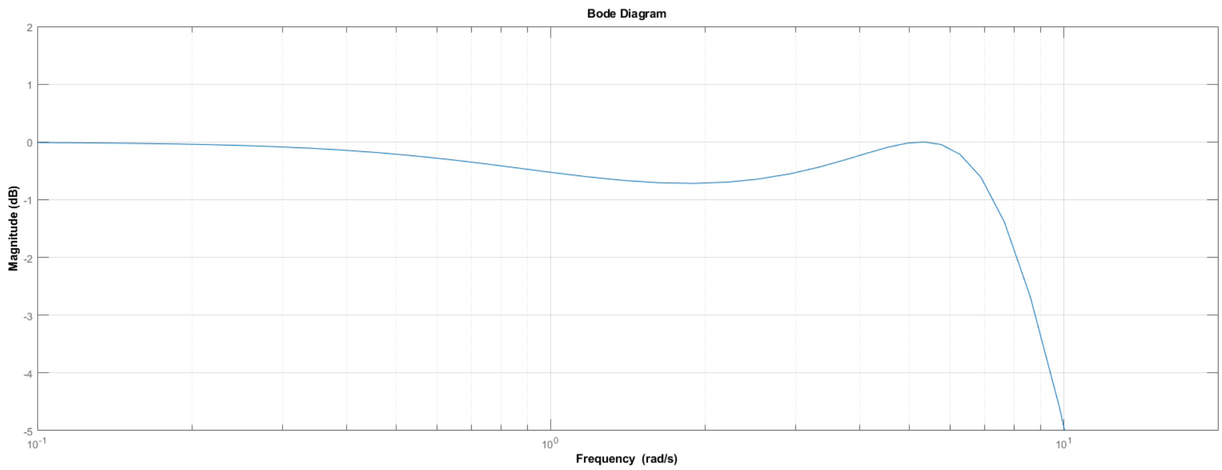

Figure 10: Desired Frequency Response Behavior of a Filter

9.1 Second Order Filter Design

Second order filters are the first possible options to be taken into account to meet the requirements stated above. The simplest second order filter has a transfer function in a form of,

$$F(s) = \frac{Kw_n^2}{s^2 + 2\xi w_n s + w_n^2} \tag{50}$$

Three parameters, namely, the unit step gain K , the natural frequency w_n and the damping ratio ξ, can be used to create wide range of second order filters.

Frequency response of the second filter can be obtained by replacing s with jw in Equation (50):

$$F(jw) = \frac{Kw_n^2}{(jw)^2 + 2\xi w_n(jw) + w_n^2} = \frac{Kw_n^2}{(w_n^2 - w^2) + 2\xi w_n wj} \tag{51}$$

The first criteria which corresponds to achieving proper unit-step response requires K to be equal to one.

The second criteria requires a magnitude gain equal to one at the frequency of disturbance such that,

$$|G(jw_d)| = \frac{w_n^2}{\sqrt{\left(w_n^2 - w_d^2\right)^2 + \left(2\xi w_n w_d\right)^2}} = 1 \tag{52}$$

With further mathematical manipulation on Equation (52), a relationship between disturbance frequency w_d, natural frequency w_n and damping ratio ξ for a suitable second order filter can be obtained as,

$$\boxed{\frac{w_d^2}{2 - 4\xi^2} = w_n^2} \tag{53}$$

Since frequency is a real property with a positive value, this requires the term $2-4\xi^2$ to be greater than zero. By simplifying this inequality, a condition for damping ratio ξ can be obtained:

$$\begin{aligned} 0 &< 2 - 4\xi^2 \\ 2\xi^2 &< 1 \\ \xi^2 &< 0.5 \end{aligned}$$

$$\boxed{\xi < 0.7071}$$

The condition for ξ states that the second order filter to be used will have an oscillatory behavior causing oscillation in the overall control as well.

9.1.1 Second Order Filter Examples

A second order filter for a disturbance frequency equal to 5.3407 rad/s was proposed in [30] as

$$F(s) = \frac{7.1155^2}{s^2 + 2\ 0.6\ 7.1155s + 7.1155^2} = \frac{50.63}{s^2 + 8.539s + 50.63} \tag{54}$$

such that its properties are consistent according to Equation (53). It can be seen that the damping ratio ξ is 0.6 and the natural frequency w_n is 7.1155 rad/s. Figure 11, 12 and 13 shows the Bode diagram, step response and graphical review of the proposed filters margin, respectively. The margins in Figure 13 were calculated using the built-in MATLAB function. As it can be seen, the MATLAB functions' phase-frequency plot has discontinuities causing unreliable comments about margins especially on phase margin.

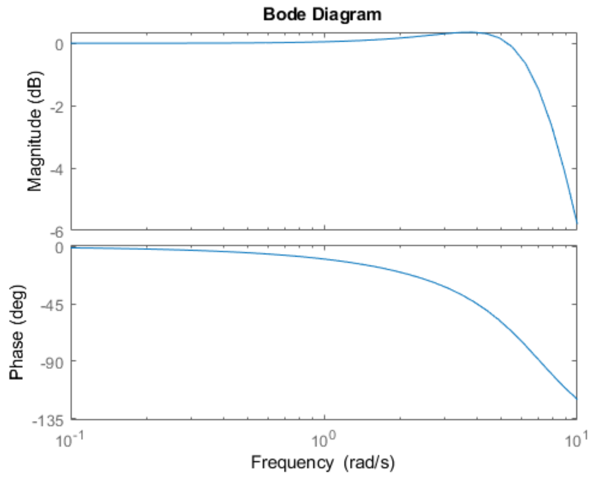

Figure 11: Frequency Response of Second-order Filter with $\xi = 0.6$, $w_n = 7.1155$

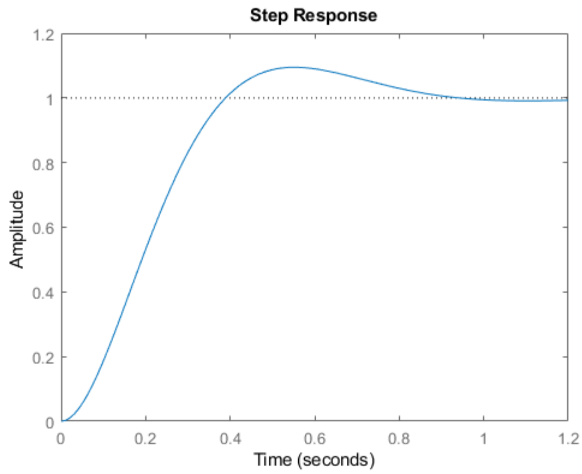

Figure 12: Unit Step Response of Second-order Filter with $\xi = 0.6$, $w_n = 7.1155$

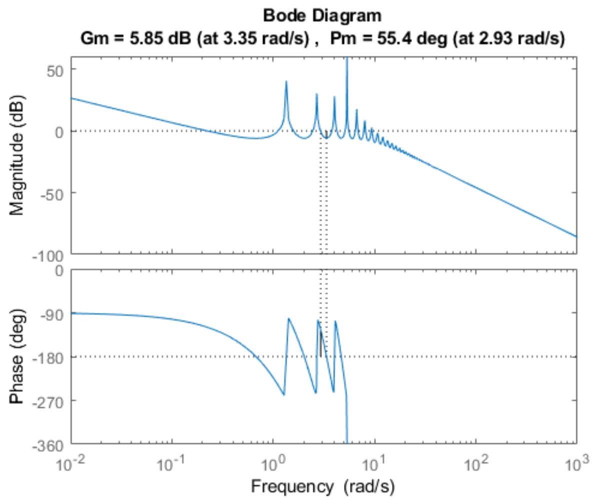

Figure 13: Gain and Phase Margin of Open-Loop Transfer Function with Second-order Filter with $\xi = 0.6$, $w_n = 7.1155$

Similar to the second order filter proposed in Equation (54), a wide range of filters for the same purpose can be generated by varying one of the parameters ξ and w_n:

9.1.2 Filter 1

Pre-selected Parameters

ξ , damping ratio = 0.3

K , unit step gain = 1

w_n ,frequency of disturbance = 5.3407 rad/s

Calculated Parameters

w_n , natural frequency = 4.1704 rad/s

Obtained Filter Transfer Function

$$F(s) = \frac{17.39}{s^2 + 2.502s + 17.39}$$

Related Graphs for Filter 1

Figure 14, 15 and 16 shows the Bode diagram, step response of Filter 1 and polar plotting of the open-loop transfer function having Filter 1, respectively.

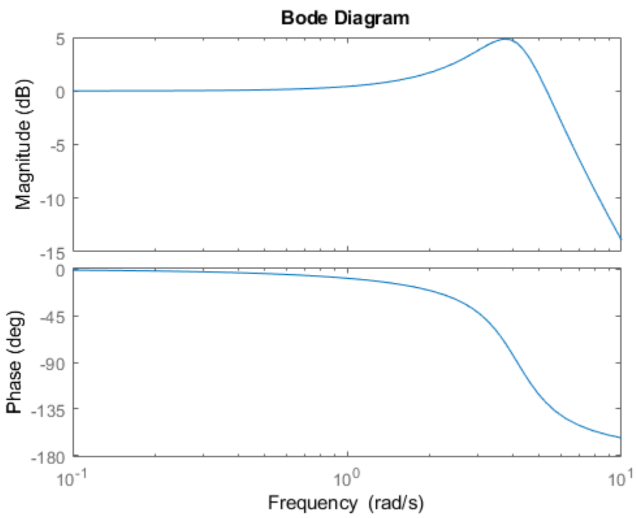

Figure 14: Frequency Response of Filter 1

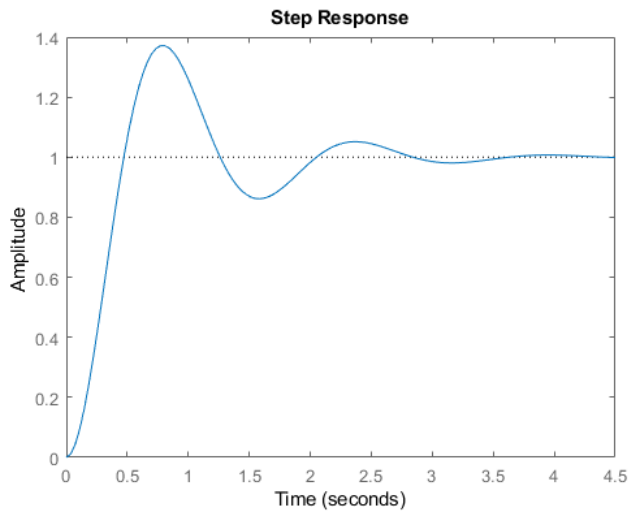

Figure 15: Unit Step Response of Filter 1

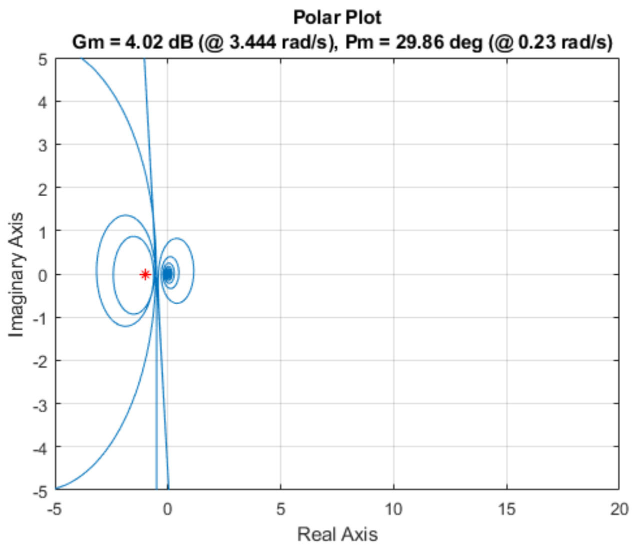

Figure 16: Gain and Phase Margin of Open-Loop Transfer Function with Filter 1

9.1.3 Filter 2

Pre-selected Parameters

ξ , damping ratio = 0.1

K , unit step gain = 1

w_n ,frequency of disturbance = 5.3407 rad/s

Calculated Parameters

w_n , natural frequency = 3.8148 rad/s

Obtained Filter Transfer Function

$$F(s) = \frac{14.55}{s^2 + 0.763s + 14.55}$$

Related Graphs for Filter 2

Figure 17, 18 and 19 shows the Bode diagram, step response of Filter 2 and polar plotting of the open-loop transfer function containing Filter 2, respectively. As expected, the decrease in damping ratio results in an increase of oscillation with respect to Filter 1.

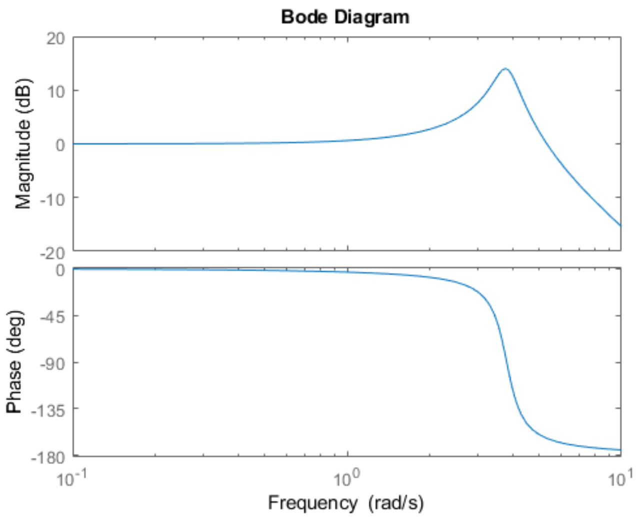

Figure 17: Frequency Response of Filter 2

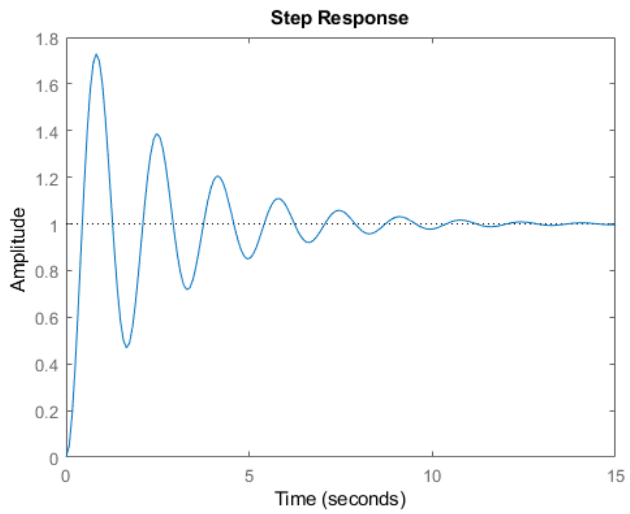

Figure 18: Unit Step Response of Filter 2

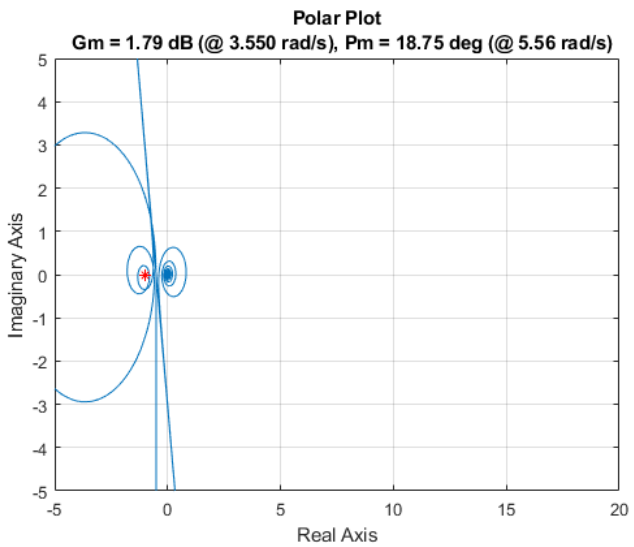

Figure 19: Gain and Phase Margin of Open-Loop Transfer Function with Filter 2

9.1.4 Filter 3

Pre-selected Parameters

ξ , damping ratio = 0.05

K , unit step gain = 1

w_n ,frequency of disturbance = 5.3407 rad/s

Calculated Parameters

w_n , natural frequency = 3.7859 rad/s

Obtained Filter Transfer Function

$$F(s) = \frac{14.33}{s^2 + 0.3786s + 14.33}$$

Related Graphs for Filter 3

Figure 20, 21 and 22 shows the Bode diagram, step response of Filter 3 and polar plotting of the open-loop transfer function containing Filter 3, respectively. As expected, the decrease in damping ratio results in an increase of oscillation with respect to Filter 1 and 2.

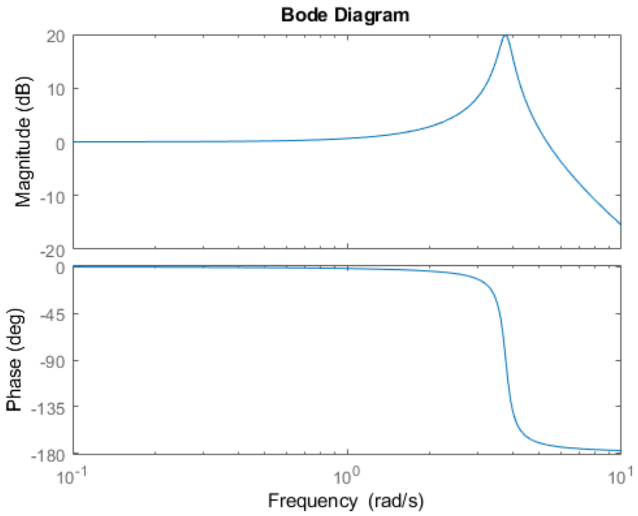

Figure 20: Frequency Response of Filter 3

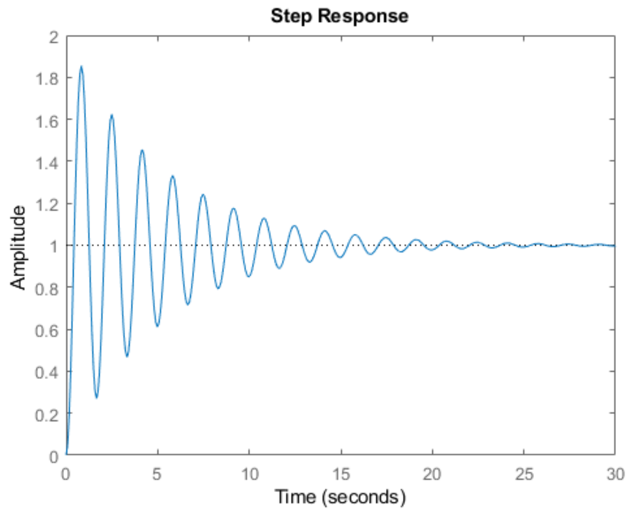

Figure 21: Unit Step Response of Filter 3

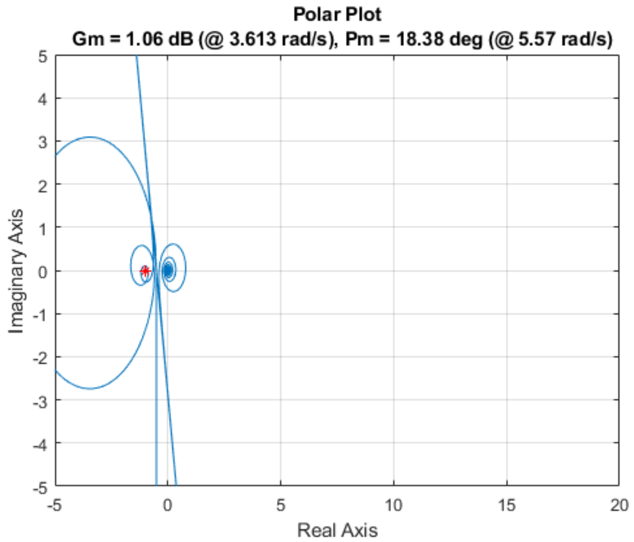

Figure 22: Gain and Phase Margin of Open-Loop Transfer Function with Filter 2

9.1.5 Filter 4

<u>Pre-selected Parameters</u>

ξ , damping ratio = 0.01

K , unit step gain = 1

w_n ,frequency of disturbance = 5.3407 rad/s

<u>Calculated Parameters</u>

w_n , natural frequency = 3.7768 rad/s

<u>Obtained Filter Transfer Function</u>

$$F(s) = \frac{14.26}{s^2 + 0.07554s + 14.26}$$

Related Graphs for Filter 4

Figure 23, 24 and 25 shows the Bode diagram, step response of Filter 4 and polar plotting of the open-loop transfer function containing Filter 4, respectively. As expected, the decrease in damping ratio results in an increase of oscillation with respect to Filter 1, 2 and 3. As it can be seen from the step response of FIlter 4, the level of oscillations and the amount of time to reach stability gives rise to really question about robustness of the controller. This expectation is supported by the decrease in gain margin as damping ratio decreases, as well.

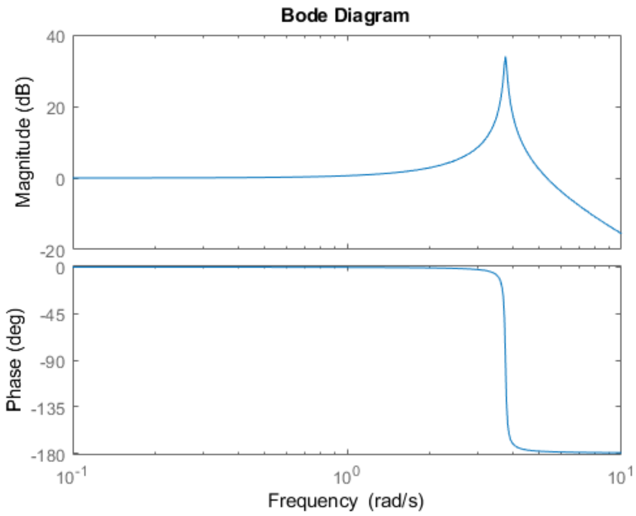

Figure 23: Frequency Response of Filter 4

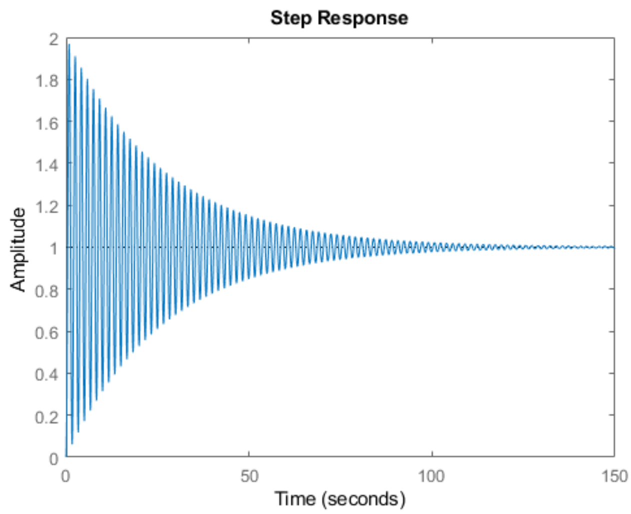

Figure 24: Unit Step Response of Filter 4

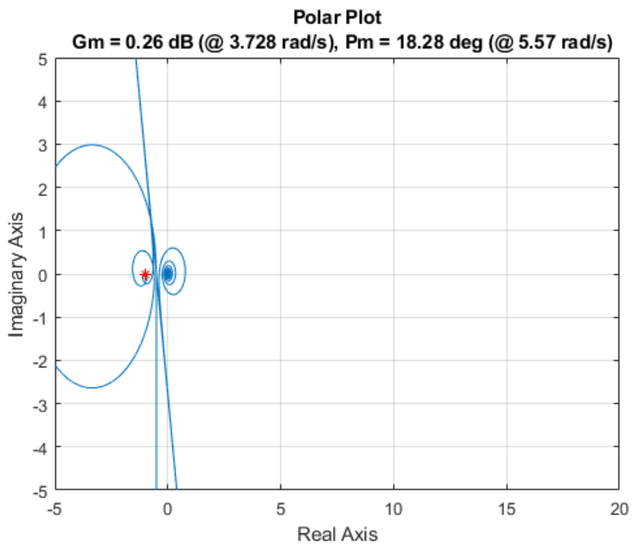

Figure 25: Gain and Phase Margin of Open-Loop Transfer Function with Filter 4

9.2 Gain Margin Variation with respect to Damping Ratio ξ when Second Order Filter is Used

The graphs in Figure 26, 27 and 28 show the influence of damping ratio on the gain margin for different disturbance frequencies and time-delay values. As a conclusion, in all cases increasing the damping ratio will increase the gain margin.

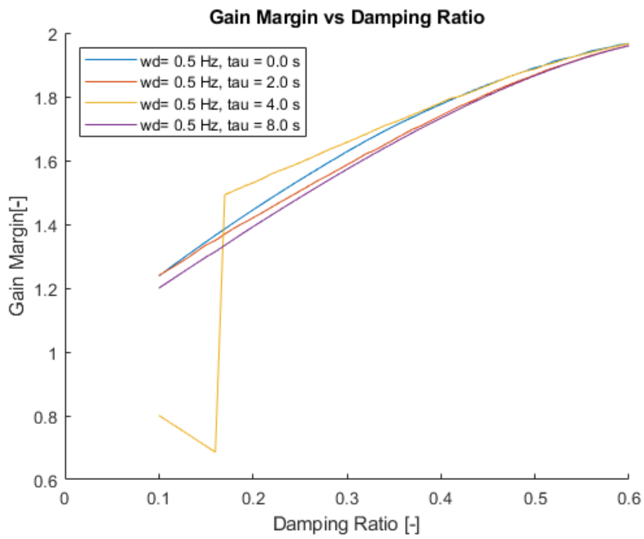

Figure 26: Gain Margin vs Damping Ratio ξ for $w_d = 0.5$ Hz

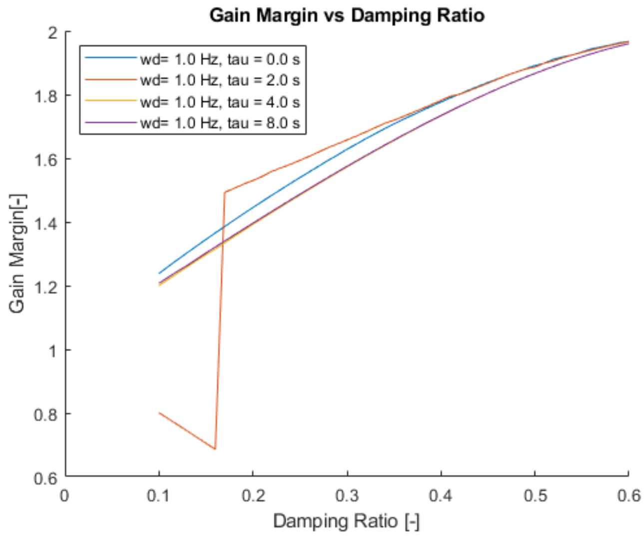

Figure 27: Gain Margin vs Damping Ratio ξ for $w_d = 1.0$ Hz

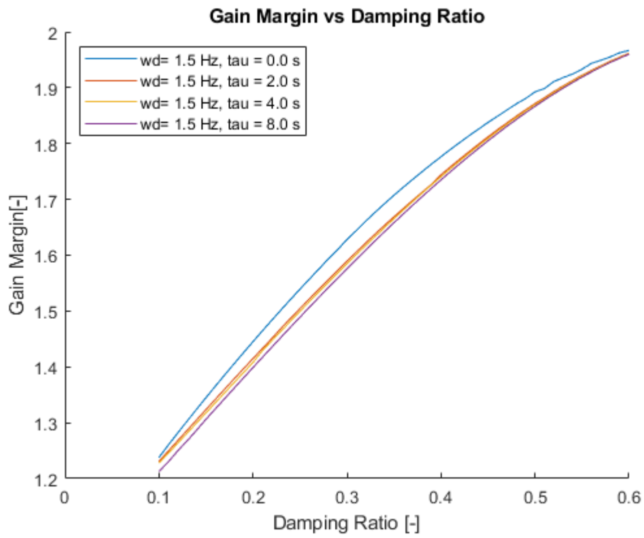

Figure 28: Gain Margin vs Damping Ratio ξ for $w_d = 1.5$ Hz

9.3 Third Order Filter Design

The methodology used to derive third order filters is based on the simple yet fundamental analysis tools provided by calculus. Even though it is possible to follow a numerical approach to find values of parameters, here an analytical approach is preferred to not to lose sight from the main mathematical idea.

As it is seen in Figure 10, the desired behavior of a filter has all of its local maximum values equal to zero decibel: first one occurring at the beginning, at which the gain corresponds to the unit step gain of the filter in decibels and the second one occurring at some frequency right before a dramatic fall.

The key idea is to first find the frequency values at which local maximums are achieved for a given form of transfer function. These frequency values will be expressed in terms of algebraic equations because this allows one to pick the frequency value where the local maximum is wanted to be observed. Once these frequencies are known, the last remaining unknown parameter is found by solving the algebraic equation that is obtained by assigning the desired gain values at these local maximums.

In this case, the filter to be designed must have a gain of 0 decibel at its local maximums. Also, it is wanted to have the second local maximum to be observed at the frequency of disturbance.

It is decided for the transfer function of the filter to have a form of,

$$F(s) = \frac{K}{T.s+1}\frac{w_n^2}{s^2+2\xi w_n s+w_n^2} \tag{55}$$

which is, basically, a combination of first and second order filter. The below explanation will show that it is possible to find a combination of such two different types of filters to give a fulfilling resultant as depicted in Figure 29.

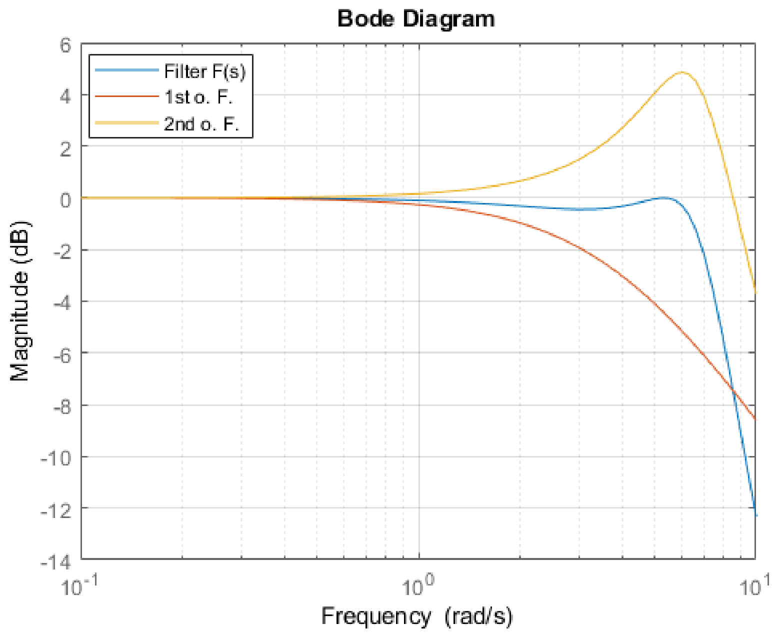

Figure 29: Resultant Filter $F(s)$ After Combination of 1^{st} and 2^{nd} Order Filter

For clarity, the first order filter part is going to be denoted by $F_1(s)$. Similarly, the second order filter part by $F_2(s)$. Hence, Equation (55) can be rewritten as,

$$F(s) = F_1(s)F_2(s) \tag{56}$$

The function for the magnitude of the frequency response can be obtained by replacing s by jw and then taking the absolute value:

$$|F(jw)| = |F_1(jw)|\,|F_2(jw)| \tag{57}$$

The extremums are found by taking the derivative of $|F(jw)|$ with respect to w and then solving for the roots:

$$\frac{d\,|F(jw)|}{dw} = \frac{d\,|F_1(jw)|}{dw}\,|F_2(s)| + |F_1(s)|\,\frac{d\,|F_2(jw)|}{dw} = 0 \tag{58}$$

With the help of MATLAB, the frequencies satisfying Equation (58) are found analytically using the command,

```
w_ext = solve(dF==0,w)
```

MATLAB returns five total solutions. One solution corresponds to w being equal to zero. Then the following two different solutions are real valued solutions. The last two solutions contain imaginary numbers; hence not realizable. So in total there exits three realizable extremum values. This is consistent with what is shown in Figure 10; it has three extremums.

The third real-valued solution corresponds to the second local maximum. Hence this is the solution that will be selected to be used in optimization. Note that, this frequency is expressed in terms of T, K, w_n and ξ.

Next, due to necessity, value assignment is made for some picked parameters, namely for K and T. It is desired to have a unit step gain equal to one. Therefore, K must be equal to one. Also, it is desired to be able to tune the filter according to an user selected time constant T. Hence a T value is also assigned.

The resonant frequency w_r is defined as the frequency at which the peak gain value is observed. In this case, it coincides with the frequency of second local maximum. It is desired that this resonant frequency is equal to the frequency of disturbance. Since the frequency of disturbance is evaluated from measurements, resonant frequency becomes a known parameter.

Until this point the unknown parameters are ξ and w_n. Also a numerical value and a symbolic representation of w_r are at disposal. When the known parameters are substituted to the symbolic representation of resonant frequency, resonant frequency becomes a function of ξ and w_n. And since the numerical value of resonant frequency is known, this function becomes an algebraic equation, allowing us to express w_n in terms of ξ.

To find the last unknown parameter ξ, an algebraic equation is formed by equating Equation (57) to one at resonant frequency w_r:

$$|F(jw_r)| = 1 \tag{59}$$

Since everything is now able to be expressed in terms of ξ, with the help of MATLAB, value of ξ can be calculated:

```
ksi_solv = solve(F1_gain*F2_gain ==1, ksi);
```

Once ξ is known, all the unknown parameters that are expressed in terms of it can be evaluated; in this particular case, w_n.

It must kept in mind that the `solve` command of MATLAB does not necessarily have to return one singular value. When one of the solutions is picked the consequence of that value must be examined through out the whole system; every calculated value must be consistent with reality.

9.4 Effectiveness of Method

The effectiveness of introduced method is demonstrated by various different filters obtained by MATLAB code working in the discussed manner.

9.4.1 Filter 5

Pre-selected Parameters

T , user-selected time-constant = 0.25 s

w_r , resonant frequency = frequency of disturbance = 5.3407 rad/s

K , unit step gain = 1

Calculated Parameters

w_n , natural frequency = 6.6726 rad/s

ξ , damping coefficient = 0.2997

Obtained Filter Transfer Function

$$F(s) = \frac{44.52}{0.25s^3 + 2s^2 + 15.13s + 44.52}$$

Related Graphs for Filter 5

Figure 30, 31 and 32 shows the Bode diagram, step response of Filter 5 and polar plotting of the open-loop transfer function containing Filter 5, respectively. When compared with Filter 1, both filters have similar response time, but Filter 5 has more oscillation. However, despite the fact there are more oscillations, due to having a upper-bounded magnitude-frequency response as seen in Figure 30, Filter 5 has a greater gain margin.

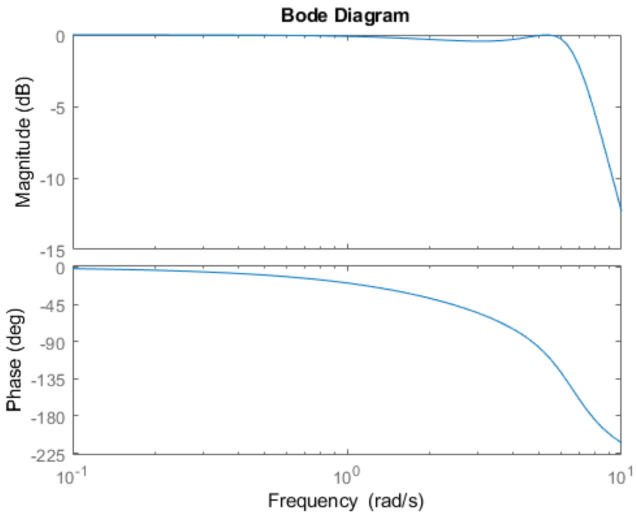

Figure 30: Frequency Response of Filter 5

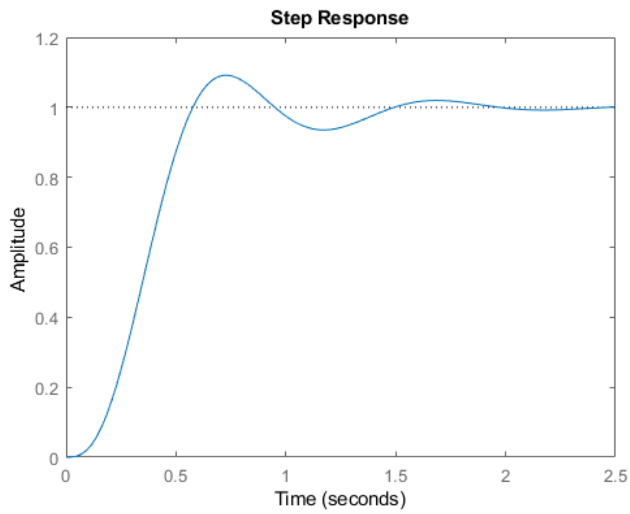

Figure 31: Unit Step Response of Filter 5

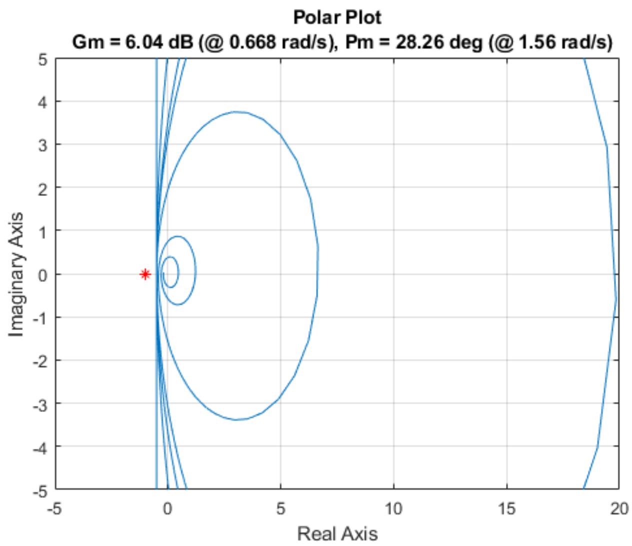

Figure 32: Gain and Phase Margin of Open-Loop Transfer Function with Filter 5

9.4.2 Filter 6

Pre-selected Parameters

T , user-selected time-constant = 0.5 s

w_r , resonant frequency = frequency of disturbance = 5.3407 rad/s

K , unit step gain = 1

Calculated Parameters

w_n , natural frequency = 5.7029 rad/s

ξ , damping coefficient = 0.1753

Obtained Filter Transfer Function

$$F(s) = \frac{32.52}{0.5s^3 + 2s^2 + 18.26s + 32.52}$$

Related Graphs for Filter 6

Figure 33, 34 and 35 shows the Bode diagram, step response of Filter 6 and polar plotting of the open-loop transfer function containing Filter 6, respectively. The increase of time constant and decrease of damping ratio, as expected, slowed down the response speed of the filter and increased the oscillations compared to Filter 5. However, as an improvement, the gain margin is increased.

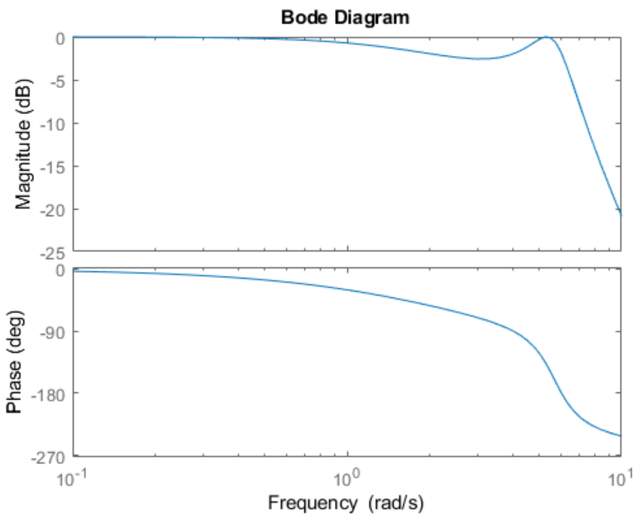

Figure 33: Frequency Response of Filter 6

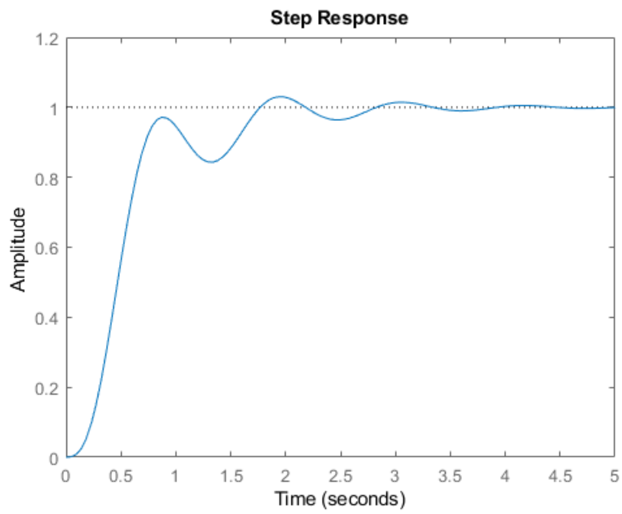

Figure 34: Unit Step Response of Filter 6

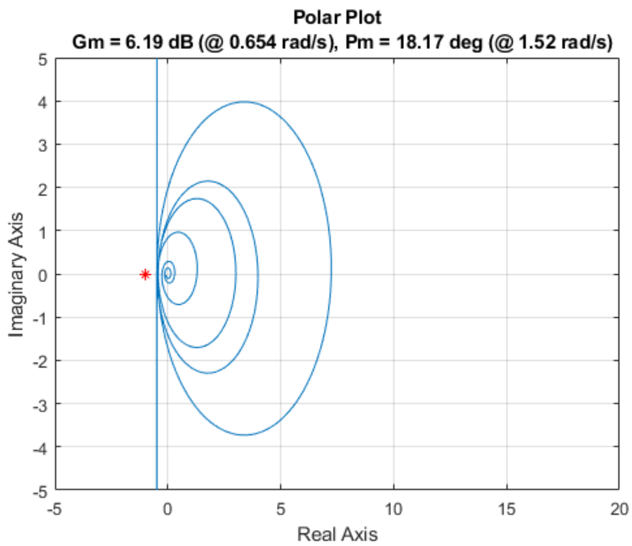

Figure 35: Gain and Phase Margin of Open-Loop Transfer Function with Filter 6

9.4.3 Filter 7

Pre-selected Parameters

T , user-selected time-constant = 2 s

w_r , resonant frequency = frequency of disturbance = 5.3407 rad/s

K , unit step gain = 1

Calculated Parameters

w_n , natural frequency = 5.3641 rad/s

ξ , damping coefficient = 0.0466

Obtained Filter Transfer Function

$$F(s) = \frac{28.77}{2s^3 + 2s^2 + 58.05s + 28.77}$$

Related Graphs for Filter 7

Figure 36, 37 and 38 shows the Bode diagram, step response of Filter 7 and polar plotting of the open-loop transfer function containing Filter 7, respectively.

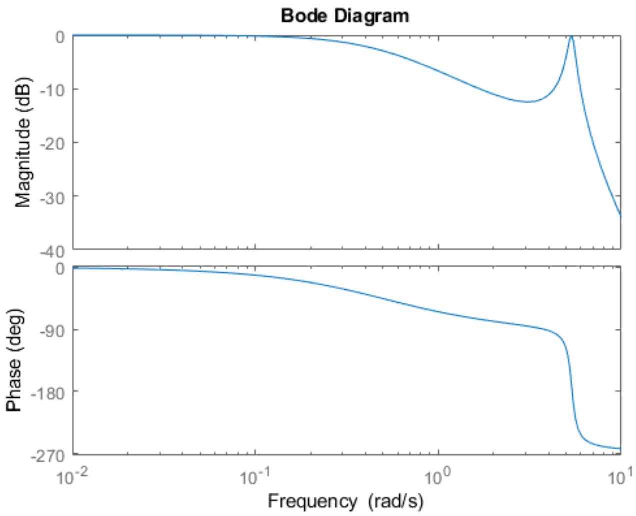

Figure 36: Frequency Response of Filter 7

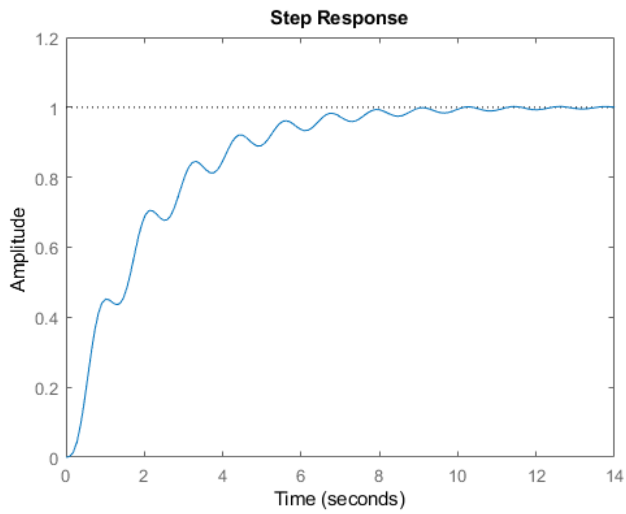

Figure 37: Unit Step Response of Filter 7

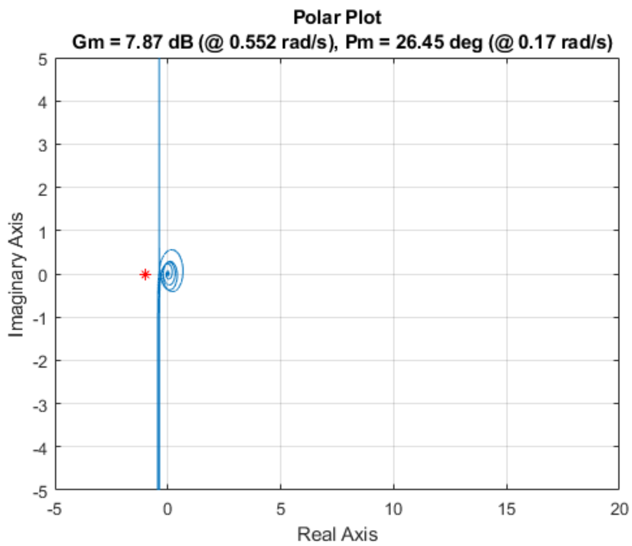

Figure 38: Gain and Phase Margin of Open-Loop Transfer Function with Filter 7

9.4.4 Filter 8

Pre-selected Parameters

T , user-selected time-constant = 4 s

w_r , resonant frequency = frequency of disturbance = 5.3407 rad/s

K , unit step gain = 1

Calculated Parameters

w_n , natural frequency = 5.3466 rad/s

ξ , damping coefficient = 0.0234

Obtained Filter Transfer Function

$$F(s) = \frac{28.59}{4s^3 + 2s^2 + 114.6s + 28.59}$$

Related Graphs for Filter 8

Figure 39, 40 and 41 shows the Bode diagram, step response of Filter 8 and polar plotting of the open-loop transfer function containing Filter 8, respectively. Contrary to the trend seen in second order filter, increment in time constant resulted in a slower and more oscillatory filter but with a great gain margin. This indicates that, using a third order filter with longer time constant will result in a more robust system even if it is oscillatory and slow. As it can be seen from the step response of the Filter 8, the response has oscillations but no overshoot.

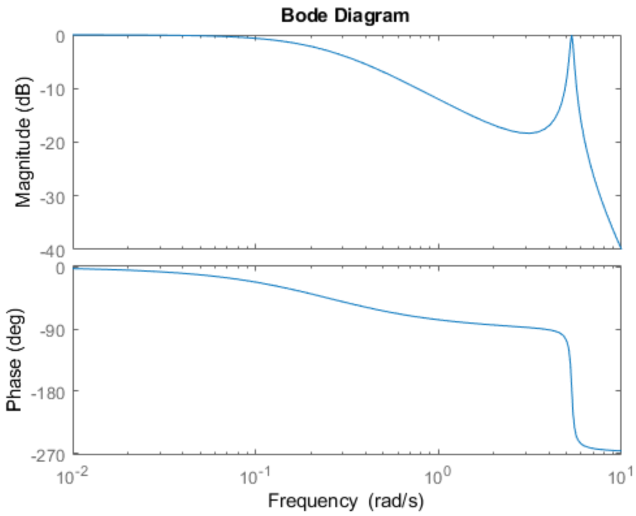

Figure 39: Frequency Response of Filter 8

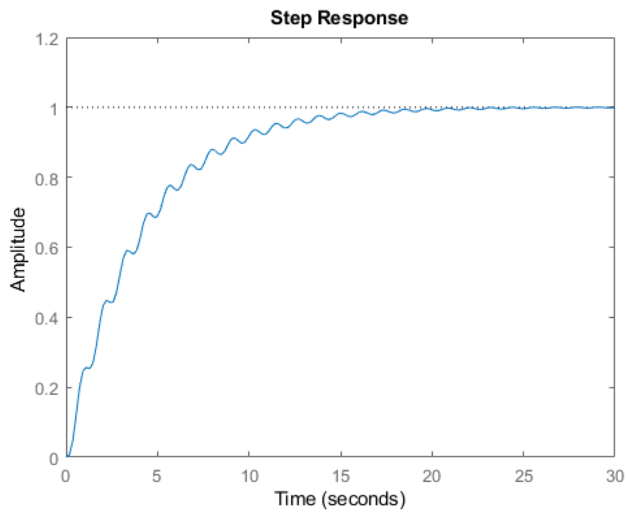

Figure 40: Unit Step Response of Filter 8

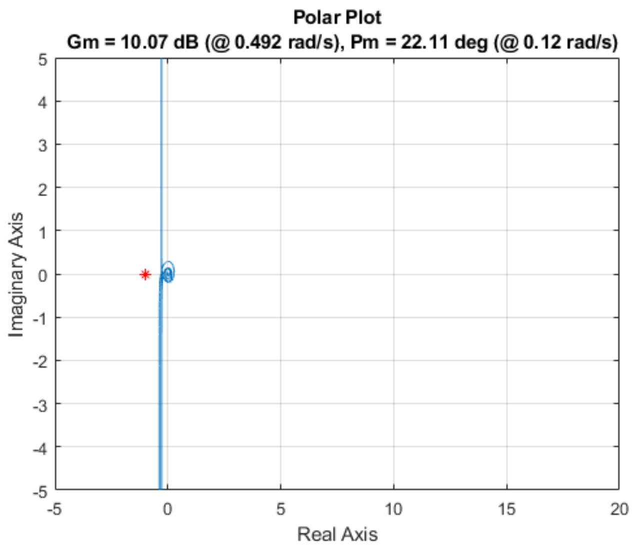

Figure 41: Gain and Phase Margin of Open-Loop Transfer Function with Filter 8

9.5 Gain and Phase Margin Variations with respect to Time-Constant T when Third Order Filter is Used

The graphs in Figure 42, 43 and 44 show the influence of time constant on the gain margin for different disturbance frequencies and time-delay values. As a conclusion, in all cases increasing the time constant will increase the gain margin. Additionally, when the system has no time-delay the gain margin increases more dramatically compared to others when time constant is change in the same amount.

The graphs in Figure 45, 46 and 47 show the influence of time constant on the phase margin for different disturbance frequencies and time-delay values. As a conclusion, in all cases increasing the time constant will decrease the phase margin and having a greater time-delay will cause the phase margin to be more resistant to the variation of time constant.

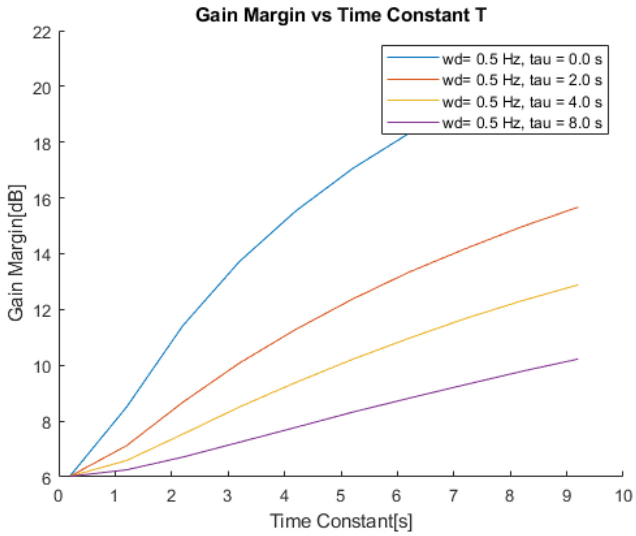

Figure 42: Gain Margin vs Time Constant T for $w_d = 0.5$ Hz

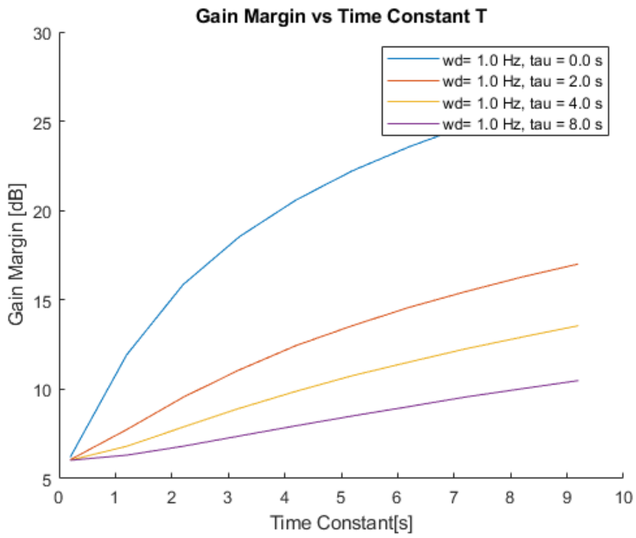

Figure 43: Gain Margin vs Time Constant T for $w_d = 1$ Hz

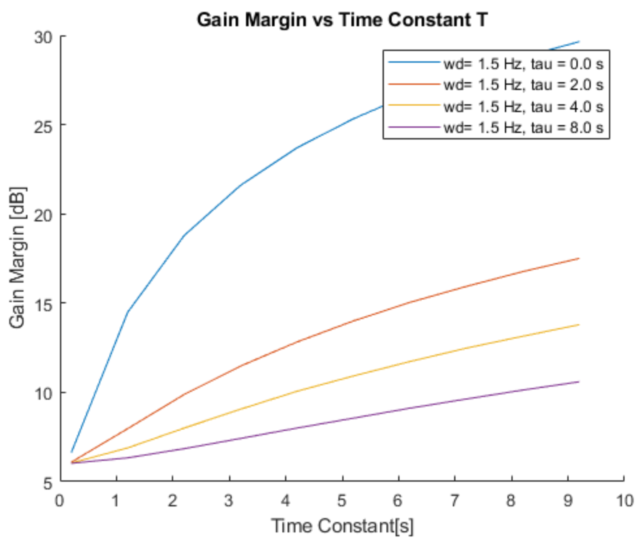

Figure 44: Gain Margin vs Time Constant T for $w_d = 1.5$ Hz

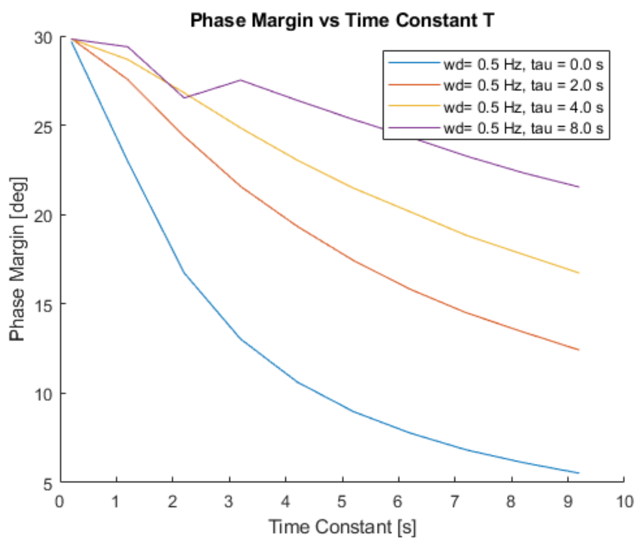

Figure 45: Phase Margin vs Time Constant T for $w_d = 0.5$ Hz

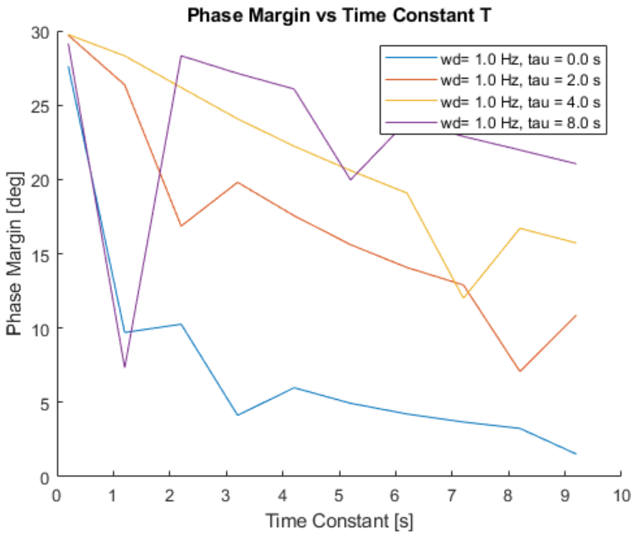

Figure 46: Phase Margin vs Time Constant T for $w_d = 1$ Hz

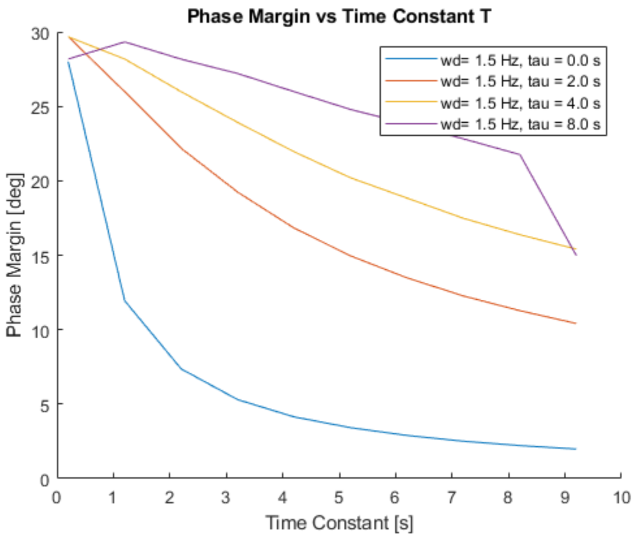

Figure 47: Phase Margin vs Time Constant T for $w_d = 1.5$ Hz

9.6 Conclusions on Third Order Filter Design

The introduced third-order filter, which is just a combination of first and second order filters, forms the simplest arrangement required to achieve the desired properties and frequency spectrum shown in Figure 10. The combined filters can provide the required frequency response behavior even though when the compound filters used standalone fail to achieve the same behavior.

In order to achieve the desired properties, ξ value of the second order filter part must have a value smaller than 0.7. This refers to that the second order filter must have an oscillatory behavior by which it also means that the resultant filter will have an oscillatory behavior. This explains why an oscillation is observed in the step response of the filter.

To reduce the oscillations in the step response, the damping factor should have a great value. The smaller the value of ξ the more the oscillation will be. However, for this specific type of transfer function form showed in Equation (55), increasing ξ results in a reduction of time constant T. Having small values of time constant causes the filter to react to any change faster.

A solution for having big ξ and T values at the same time, could be to introduce a zero to the transfer function in Equation (55):

$$F(s) = \frac{K}{T_2.s+1}\frac{w_n^2}{s^2+2\xi w_n s+w_n^2}\frac{T_1 s+1}{1} \tag{60}$$

The introduced new zero brings a new parameter value that can be optimized to achieve desired values of ξ and T simultaneously. However, substitution of this new zero brings more computational difficulties in evaluation of the filter parameters. For instance, to find the extremum points the equation,

$$\frac{d\,|F(jw)|}{dw} = \left(\frac{d\,|F_1(jw)|}{dw}\,|F_2(s)| + |F_1(s)|\,\frac{d\,|F_2(jw)|}{dw}\right)|F_3(jw)| + |F_1(jw)|\,|F_2(jw)|\,\frac{d\,|F_3(jw)|}{dw} = 0$$

must be solved. Here, $F_3(s)$ denotes the introduced zero.

9.7 Important Remarks

Theoretically, the filter design methodology discussed above can be applied to all forms of filter transfer functions having an order greater than two. It must be kept in mind though, that for filters with great order, the evaluation of the parameters may be possible only by numerical calculations, not by symbolic manipulation.

However, the decision of the transfer function must be done with respect to two aspects:

First of all, the number of poles that the filter has must be greater than the number of poles that the plant to be controlled has.

Second, the number of zeros that can be introduced to the filter can not exceed the result of the difference,

$$N_Z = N_P - R.O.P \tag{61}$$

where N_Z and N_P denotes the number of zeros and poles that the filter has, respectively. Additionally, $R.O.P$ stands for the Relative Order of Plant.

These two conditions assures the controller to be causal, or in other words, physically realizable.

10 Numerical Simulations

Other than frequency analysis, to have an information about the whole IMC systems time-domain performance, the system introduced in Figure 1 is implemented to a computer simulation program, in this case, MATLAB/Simulink.

For evaluation of the effectiveness of the introduced control strategy, a basic block model of an IMC system is created in MATLAB/Simulink as shown in Figure 48.

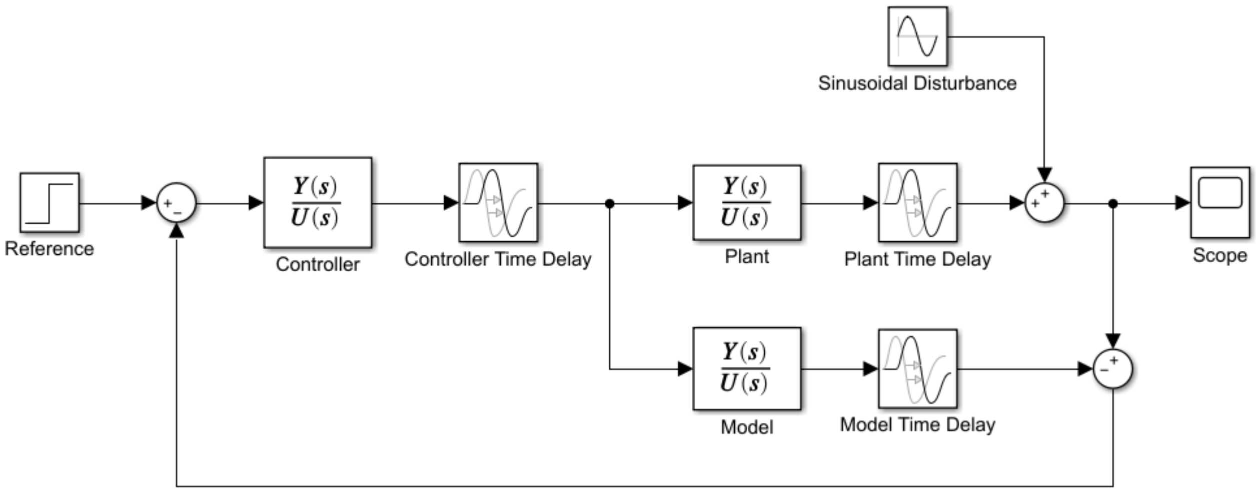

Figure 48: Block Model of an IMC system in Matlab/Simulink

The block model representation of the system allows easy setting of the system and good visualization. The controller block depicted in Figure 48 comprises the IMC controller without the time-delay component; the user-definable time delay component is introduced in the controller time delay block. The filter models generated by the MAT-

LAB script that tunes the filters for IMC and disturbance rejection, can be directly implemented to the controller block. This fact allows smoothness and fastness in the evaluation of the time-domain performance of the system in simulation.

In this thesis, the system and model time-delays are assumed to be equal to each other.

Using the block model in Figure 48, four different IMC controllers are tested and their performances are compared for two cases to demonstrate the robustness of an example system. The first case is when there exists no mismatch between the plant and model; the second case is when there exists mismatch:

10.1 Case 1: No Plant-Model Mismatch

Plant Transfer Function :

$$G(s) = \frac{0.5}{0.5s + 1}e^{-4s}$$

Model Transfer Function :

$$\tilde{G}(s) = \frac{0.5}{0.5s + 1}e^{-4s}$$

Figure 49 shows four internal model control systems with different filters, having no plant/model mismatch, subjected to periodic disturbance and a reference value of 0.1. This case corresponds to the ideal case were all assumptions are satisfied. Therefore, every internal model control system tuned with respect to the criteria will work perfectly. In this case, gain margin does not bring any advantage at all to consider for system response. As it can be seen, the third order filter with four seconds of time constant is not preferable even if it has the biggest gain margin among all the other filters.

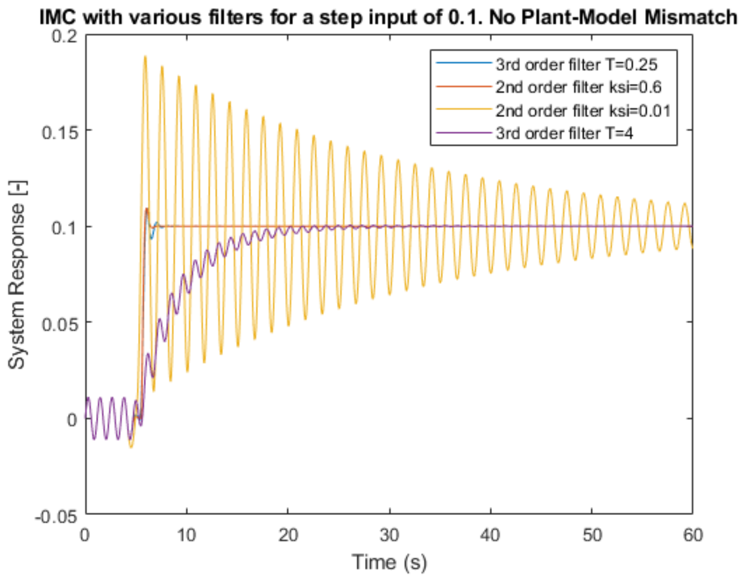

Figure 49: IMC realized with four different filters with plant-model mismatch

10.2 Case 2: With Plant-Model Mismatch

Plant Transfer Function :

$$G(s) = \frac{0.5}{0.2s + 1}e^{-4s}$$

Model Transfer Function :

$$\tilde{G}(s) = \frac{0.5}{0.5s + 1}e^{-4s}$$

Figure 50 shows four internal model control systems with different filters, having plant/model mismatch, subjected to periodic disturbance and a reference value of 0.1. In this case the assumptions are not completely valid and robustness becomes an important property to be considered. As it can be seen, the IMC system with the third order filter with four seconds of time constant is the only one that accomplishes the control task. Despite it is still slow and oscillatory, having a large gain margin lets the system to keep its stability and control capability.

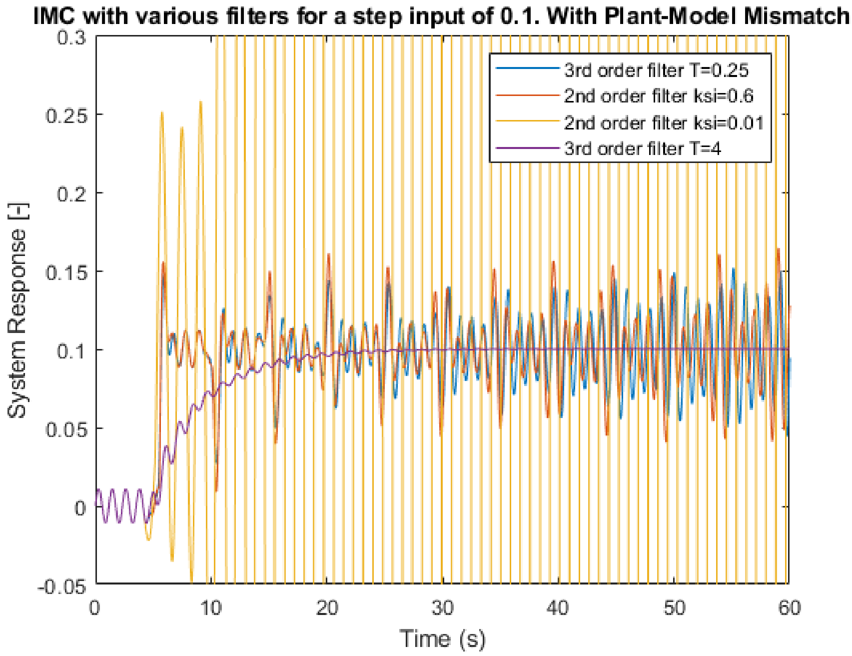

Figure 50: IMC realized with four different filters with plant-model mismatch

11 Conclusions

Experimental identification of a hot rolling mill can be sufficiently made by assuming a first order model with time-delay. The method used in the thesis first evaluates the information of the time-delay and then the parameters. The method shows the validity and simplicity of using correlation and ARMAX modeling for identification. However, compared to todays methods, the used method can be slow and very much limited. With further mathematical manipulation all the parameters are evaluated for the system and the disturbance. For effective identification, the data at disposal must contain various changes of input and output; identification from steady-state responses are not convenient.

In the presence of sinusoidal disturbance, internal model control strategy gives a promising solution to achieve successful reference tracking and rejection of the disturbance even when the system to be controlled has inherent time-delays. With a consistent model of the real system being at disposal, the theory and simulations show that the controller meets the expectancy in the means of control, even when there is a slight difference between the real system and model.

However, the thesis also concludes with an important fact that the level of this difference that the controller can tolerate, varies with respect to the type of filter used in the internal model control. Even though the second order filter seems to be the simplest filter that fulfills all the criterias demanded by the internal model control, the applicability of this type of filter becomes questionable when there exists a mismatch between model and system.

To bring an enhancement to the applicability of the control method, third order filters which are developed by combining first and second order filters are introduced. An algorithm that tunes the parameters of third order filters according to the conditions and limitations set for the purpose of optimization, generates filters that result in a more robust control than second order filters can offer. However, using the introduced third-order filters brings oscillation problems due to the fact that the new filters have low damping-ratios.

Fortunately, the third order filter model in this thesis includes, additional to second order filters, a parameter, specifically the time constant, to be defined by the user. This feature lets the user to choose the best setting of exchange between robustness and responsiveness of the system making the introduced third order filters more applicable.

The thesis shows that more effective quantification of robustness is needed to have a better design paradigm and comparison of filters. Such techniques like H_∞ optimization may provide more benefits for the robustness of control system.

References

[1] Jan Swevers. Internal model control (imc). *Control Theory*, 2006.

[2] Roland Heeg, Andreas Kugi, Olivier Fichet, Laurent Irastorza, and Christophe Pelletier. Modeling and control of plate thickness in hot rolling mills. *IFAC Proceedings Volumes*, 38(1):13–18, 2005.

[3] A Kovari and D Fodor. Simulation of rolling mill's electro-hydraulic gap adjustment system. In *2012 IEEE 13th International Symposium on Computational Intelligence and Informatics (CINTI)*, pages 377–380. IEEE, 2012.

[4] Maciej Pietrzyk and John G Lenard. *Thermal-mechanical modelling of the flat rolling process*. Springer Science & Business Media, 2012.

[5] Yucai Zhu. *Multivariable system identification for process control*. Elsevier, 2001.

[6] S Ahmed, B Huang, and SL Shah. Parameter and delay estimation of continuous-time models using a linear filter. *Journal of Process Control*, 16(4):323–331, 2006.

[7] Jean-Pierre Richard. Time-delay systems: an overview of some recent advances and open problems. *automatica*, 39(10):1667–1694, 2003.

[8] Ashraf Elnaggar, Guy A Dumont, and A-L Elshafei. Recursive estimation for system of unknown delay. In *Proceedings of the*

28th IEEE Conference on Decision and Control,, pages 1809–1810. IEEE, 1989.

[9] Kamali Marzieh, Askari Javad, et al. Parametric identification of input-delay systems with unknown time delay. In *2007 Chinese Control Conference*, pages 246–250. IEEE, 2007.

[10] FG Rossomando and J Denti Filho. Modelling and control of a hot rolling mill. *Latin American applied research*, 36(3):199–204, 2006.

[11] Kazuki Omura, Hiroto Ujikawa, Osamu Kaneko, Yuki Okano, Shigeru Yamamoto, Hiroyuki Imanari, and Tokujiro Horikawa. Attenuation of roll eccentric disturbance by modified repetitive controllers for steel strip process with transport time delay. *IFAC-PapersOnLine*, 48(17):131–136, 2015.

[12] SS Garimella and K Srinivasan. Application of repetitive control to eccentricity compensation in rolling. In *Proceedings of 1994 American Control Conference-ACC'94*, volume 3, pages 2904–2908. IEEE, 1994.

[13] Shinji Hara, Yutaka Yamamoto, Tohru Omata, and Michio Nakano. Repetitive control system: A new type servo system for periodic exogenous signals. *IEEE Transactions on automatic control*, 33(7):659–668, 1988.

[14] A.V. Oppenheim, A.S. Willsky, and S.H. Nawab. *Signals and Systems*. Prentice-Hall signal processing series. Prentice Hall, 1997.

[15] Katsuhiko Ogata and Yanjuan Yang. *Modern control engineering*, volume 4. Prentice-Hall, 2002.

[16] Sigurd Skogestad and Ian Postlethwaite. *Multivariable feedback control: analysis and design*, volume 2. Wiley New York, 2007.

[17] Brad Osgood. The fourier transform and its applications. *Lecture notes for EE*, 261:20, 2009.

[18] Rifat Sipahi, Tomáš Vyhlídal, Silviu-Iulian Niculescu, and Pierdomenico Pepe. *Time delay systems: Methods, applications and new trends*, volume 423. Springer, 2012.

[19] Wei Xing Zheng. On least-squares identification of armax models. *IFAC Proceedings Volumes*, 35(1):391–396, 2002.

[20] Milan Hofreiter. *Identifikace systemu I*. CVUT, 2009.

[21] Peter Young. Parameter estimation for continuous-time models—a survey. *Automatica*, 17(1):23–39, 1981.

[22] Jean-Jacques E Slotine, Weiping Li, et al. *Applied nonlinear control*, volume 199. Prentice hall Englewood Cliffs, NJ, 1991.

[23] Jeremy Orloff. Topic 11 notes: Argument principle. *MIT Class Notes of 18.04*.

[24] Norman S Nise. *Control System Engineering*. John Wiley & Sons, 2007.

[25] Bruce A Francis and Walter Murray Wonham. The internal model principle of control theory. *Automatica*, 12(5):457–465, 1976.

[26] Daniel E Rivera. Internal model control: a comprehensive view. *Arizona State University*, 1999.

[27] Youqing Wang, Furong Gao, and Francis J Doyle III. Survey on iterative learning control, repetitive control, and run-to-run control. *Journal of Process Control*, 19(10):1589–1600, 2009.

[28] Gunnar Hillerström and Kirthi Walgama. Repetitive control theory and applications-a survey. *IFAC Proceedings Volumes*, 29(1):1446–1451, 1996.

[29] Manfred Morari and Evanghelos Zafiriou. *Robust process control*. Morari, 1989.

[30] Mert Okar. Time delay compensation algorithms for rolling mills. *Diploma Thesis*, 2017.

[31] Charles Knapp and Glifford Carter. The generalized correlation method for estimation of time delay. *IEEE transactions on acoustics, speech, and signal processing*, 24(4):320–327, 1976.

[32] Lennart Ljung. Experiments with identification of continuous time models. *IFAC Proceedings Volumes*, 42(10):1175–1180, 2009.